Research Square

Preprints are preliminary reports that have not undergone peer review.
They should not be considered conclusive, used to inform clinical practice,
or referenced by the media as validated information.

Model-free tunable predefined-time stable time-delay attitude control of satellites using exponential Lyapunov rule and time delay estimation based uncertainty compensation

Ahmadreza Karemi
Malek Ashtar University of Technology
Mahdi Jafari
m.jafari.h@mut.ac.ir
Malek Ashtar University of Technology
Alireza Ahangarani Farahani
Malek Ashtar University of Technology

Research Article

Keywords: Attitude control, satellite, predefined-time stability, sliding mode control, time delay estimation, model-free

Posted Date: November 19th, 2026

DOI: https://doi.org/10.21203/rs.3.rs-11494754/v1

License: This work is licensed under a Creative Commons Attribution 4.0 International License.
Read Full License

Additional Declarations: No competing interests reported.

Model-free tunable predefined-time stable time-delay attitude control of satellites using exponential Lyapunov rule and time delay estimation based uncertainty compensation

Ahmadreza Karemi [1], Mahdi Jafari [2]*, Alireza Ahangarani Farahani[3]

1. Ph.D. student of Aerospace engineering, University of Malek-e-Ashtar, Tehran, Iran,
2. Associate professor of Aerospace engineering, University of Malek-e-Ashtar, Tehran, Iran
3. Assistant Professor of Aerospace engineering, University of Malek-e-Ashtar, Tehran, Iran

Corresponding Author Email; m.jafari.h@mut.ac.ir

Abstract: This paper proposes a model-free, predefined-time attitude control framework for satellites operating in the presence of parametric uncertainties and external disturbances. In contrast to existing predefined-time control methods, which are often developed on the basis of restrictive Lyapunov structures and model-dependent disturbance estimation schemes, a novel predefined-time Lyapunov function with enhanced parametric flexibility is first formulated. The proposed Lyapunov framework enables explicit adjustment of the transient response while ensuring predefined-time convergence under practical operating conditions characterized by lumped uncertainties and unknown disturbance torques. To compensate for the aggregated uncertainty without requiring precise knowledge of the satellite inertia parameters or prior information regarding disturbance bounds, a time-delay estimation (TDE) mechanism is incorporated into the control architecture. This leads to a genuinely model-free predefined-time sliding mode controller. Rigorous stability analysis establishes the boundedness of all closed-loop signals and proves that the attitude-tracking errors converge to zero within the prescribed settling time, independently of the initial conditions. Finally, simulation studies conducted for a satellite attitude-control scenario demonstrate the effectiveness, robustness, and rapid convergence of the proposed method in comparison with existing control approaches.

Keywords: Attitude control, satellite, predefined-time stability, sliding mode control, time delay estimation, model-free

1. Introduction

Precise satellite attitude control is regarded as one of the most fundamental and, at the same time, most critical subsystems in modern spacecraft engineering [1], [2], [3]. The angular attitude of a satellite directly determines the orientation of its payloads, antennas, solar arrays, and sensors with respect to inertial or orbital reference frames, and therefore plays a decisive role in the success of missions such as Earth remote sensing, space exploration, communication satellites, formation flying, rendezvous and proximity operations, and on-orbit servicing [2], [3]. Even very small attitude deviations may lead to severe performance degradation, including communication link interruption, reduced pointing accuracy of optical sensors, loss of power generation efficiency, and ultimately an increase in the overall mission risk. Since today's space missions increasingly require higher precision, faster maneuverability, and greater robustness against environmental uncertainties, the development of reliable and high-performance solutions for satellite attitude control has become an increasingly essential and challenging task [2], [3].

From a dynamical viewpoint, satellite attitude motion is inherently nonlinear, coupled, and complex, and is strongly affected by various types of uncertainties and external disturbances. Parametric uncertainties usually arise from imperfect knowledge of the inertia matrix, which may result from factors such as manufacturing tolerances, fuel consumption, fuel sloshing, the presence of flexible structures, deployment of foldable appendages, or payload configuration changes throughout the mission lifetime. In addition, unmodeled dynamics such as structural vibrations, actuator dynamics, sensing delays, and friction effects further complicate the accurate modeling of attitude dynamics [4], [5], [6], [7]. Along with these internal factors, satellites are constantly subjected to external disturbance torques, including gravity-gradient effects, aerodynamic drag in low Earth orbits, solar radiation pressure, residual magnetic torques, and thermal radiation-induced forces. These disturbances are often time-varying, partially unpredictable, and difficult to bound accurately, particularly in long-duration missions or dynamic operational scenarios.

Consequently, the performance of an attitude control system is not limited merely to its nominal tracking capability, but also depends on its robustness against uncertainties and disturbances. High-accuracy attitude control requires that, in addition to fast and precise tracking of desired trajectories, effective mechanisms be incorporated to identify, estimate, and compensate for the aggregated effects of modeling errors and external disturbances. In the absence of such mechanisms, controller design must resort to very large gains or conservative disturbance bounds, which may lead to actuator saturation, high energy consumption, chattering, and even system instability [4], [5].

From this perspective, disturbance and uncertainty estimation plays a central role in satellite attitude control design. Rather than relying on exact knowledge of system parameters or pessimistic assumptions, modern robust control frameworks often employ the concept of a "lumped uncertainty," meaning that all unknown dynamics, parametric uncertainties, and external disturbances are modeled as a unified equivalent disturbance term [2]. Accurate online estimation of this term enables the controller to actively compensate for its effects, thereby significantly improving tracking accuracy and system robustness without excessive conservatism in design. The effectiveness of this estimation process is particularly critical in applications requiring fast transient response and high precision, where it has a decisive impact on closed-loop performance.

For the core control architecture, sliding mode control has emerged as one of the most effective approaches, mainly due to its inherent robustness and strong capability in handling nonlinear dynamics [8], [9]. One of the key advantages of sliding mode in satellite attitude control is its robustness against model uncertainties and external disturbances [8], [9], [10]. Since satellite dynamics are highly nonlinear and often time-varying, maintaining precise control is inherently challenging. Sliding mode addresses this issue by forcing the system trajectories onto a carefully designed sliding surface, which is formulated to attenuate disturbances and compensate for modeling errors. Once the system reaches this surface, the controller ensures that it remains on it, thereby minimizing the adverse effects of uncertainties and disturbances.

Compared with other advanced methods such as optimal control, model predictive control, backstepping, or adaptive control, the design and implementation of sliding mode control is relatively simpler. This method mainly requires the definition of a suitable sliding surface and a control law, which makes it computationally efficient—a matter of particular importance for on-board satellite systems with limited processing resources. Furthermore, sliding mode is inherently well suited for handling nonlinearities arising not only from environmental conditions but also from internal system variations, including inertia variations due to fuel consumption. This capability is essential for guaranteeing long-term accuracy in satellite attitude stabilization, especially in missions where the system faces considerable uncertainties [3].

Sliding-mode-based systems are capable of achieving various forms of stability, including asymptotic stability, finite-time stability, fixed-time stability, and the more recent concept of predefined-time stability. Each of these stability frameworks has its own specific characteristics, advantages, and limitations.

Earlier investigations into spacecraft attitude control predominantly focused on asymptotic convergence frameworks. Aleksandrov and Tikhonov [11] investigated a PID-like controller for triaxial electrodynamic attitude stabilization in orbital frames, whereas Lee [12] utilized a nonlinear disturbance observer-based robust control to compensate for environmental torques. Baghi et al. [13] developed a nonlinear PD controller targeting the three-axis stabilization of flexible satellites, and Yao [14] introduced a robust adaptive iterative learning control scheme to improve high-precision tracking over repeated maneuvers. Despite achieving asymptotic stability, these methodologies cannot ensure convergence within a limited duration. To address this limitation, finite-time (FT) approaches were established; Guo et al. [15] developed an integral sliding mode attitude controller under actuator saturation, Ezabadi and Emami [16] synthesized a composite-learning-based fault-tolerant FT scheme under inertia uncertainties and disturbances, and Yao [17] designed a robust FT stabilization method capable of attenuating attitude measurement uncertainties. Nevertheless, the settling time in FT techniques strictly depends on the initial conditions, which can lead to excessively slow responses during large-angle maneuvers.

To overcome the initial-condition dependency of FT convergence, fixed-time (FxT) control schemes were developed. Guan et al. [18] constructed an adaptive FxT sliding mode controller for reorientation under pointing constraints, while Zhuang and Song [19] addressed actuator torque saturation via a fault-tolerant FxT architecture. Bingöl [20] incorporated neural networks into FxT sliding mode control for chaotic satellite dynamics, Barman and Sinha [21] introduced a nonsingular fast FxT sliding surface to accelerate convergence, and Golestani et al. [22] formulated an FxT attitude controller for flexible spacecraft vibration suppression. Although FxT control ensures an upper bound on settling time, this bound is often conservative and cannot be arbitrarily predetermined. Consequently, predefined-time (PT) control was proposed to directly tune the convergence time as a prior parameter. Wang et al. [31] presented baseline PT attitude stabilization for rigid spacecraft, while Ye et al. [23] achieved predefined-time predefined-bounded tracking. Tunable settling times were further realized by Wu et al. [24], and distributed PT consensus for multiple spacecraft was formulated by Sun et al. [25]. Furthermore, Xie et al. [26] developed an approximation-free PT attitude control scheme under state constraints, Su and Shen [27] proposed an adaptive fault-tolerant PT framework with guaranteed performance, and Xie and Chen [28] constructed a nonsingular adaptive PT controller. More recently, Xiao et al. [29] realized continuous nonsingular PT tracking for flexible platforms, and Xu et al. [30] resolved the actuator saturation issue while preventing unwinding maneuvers under predefined time constraints.

To effectively handle complex disturbances and unmeasurable states in practical aerospace applications, PT frameworks have been coupled with advanced observers and intelligent estimators. In observer-based developments, Zhang et al. [32] validated an experimental disturbance-observer-based PT attitude tracking scheme, Ye et al. [33] introduced an extended-state observer (ESO) enabling velocity-free PT control, and Xuan-Mung et al. [34] designed an observer-based PT scheme capable of rejecting arbitrary external disturbances. Chen et al. [35] developed a nonsingular sliding mode attitude stabilizer supported by a PT observer, Zheng et al. [36] formulated an attitude tracking controller with simultaneous disturbance estimation, and Xie and Chen [37] integrated PT disturbance estimation with attitude control. In parallel, intelligent learning-based PT controllers have been advanced; Zhang et al. [38] combined neural networks with PT control to approximate unknown dynamics, and Lu et al. [39] designed a neural-network-observer-based PT controller for morphing hypersonic configurations. Finally, to manage severe non-smooth system constraints and uncertainties, Xie et al. [40] developed an adaptive fuzzy PT dynamic surface control method under state constraints, and Xu et al. [41] formulated a fuzzy adaptive PT tracking architecture with asymptotic error performance.

To provide a clearer comparison among these stability concepts, their main features are described separately in the following paragraphs.

Asymptotic stability: In this case, the system states gradually tend toward the equilibrium point over time and converge to it in the limit of infinite time. Although the design and analysis of this type of stability is relatively straightforward, its main limitation is the absence of any guarantee concerning the convergence time, and the convergence process may be very slow. In real-time satellite operations, where in some cases a fast response is critical for mission success, this shortcoming can become a significant limitation.

Finite-time stability: In this framework, the system reaches a stable state within a finite time interval with certainty. However, the duration of this time depends on the initial conditions of the system. Although this method provides a faster convergence rate than asymptotic stability, its dependence on the initial states makes it less suitable for conditions accompanied by significant uncertainty or variability—a situation frequently observed in satellite dynamics.

Fixed-time stability: In this framework, the system converges within a fixed time that is independent of the initial conditions and is determined solely by the controller design parameters. This property makes it very attractive for real-time systems with stringent timing constraints. However, the design process becomes more complex and requires careful tuning of the parameters so as to guarantee both system robustness and the desired performance.

Predefined-time stability: This concept advances fixed-time control by allowing the designer to explicitly determine the convergence time from the very beginning of the control process. Unlike finite-time or fixed-time methods, predefined-time stability provides both a convergence guarantee and an exact bound on the required time. This property is particularly beneficial for critical satellite operations that require precise timing and synchronization, since it enables the controller to reliably adhere to strict operational deadlines.

The application of predefined-time stability to satellite attitude control offers several key advantages that make it highly attractive for space missions. Some of the most important of these advantages are presented below [27], [35], [41]:

1. Precise timing requirements

Many space missions, such as Earth observation and astronomical imaging, require precise temporal coordination for tasks such as data acquisition and sensor alignment. In such applications, the existence of a certain and predictable convergence time is essential so that attitude stabilization is carried out within predefined operational windows and that both mission planning and the simultaneous operation of multiple sensors are guaranteed reliably.

2. Performance assurance in critical mission phases

Space missions often involve critical phases such as launch, orbital injection, or delicate maneuvers, in which fast and accurate attitude alignment is essential. By requiring convergence within a specified time interval, predefined-time stability guarantees that the spacecraft attains the required orientation without delay, thereby ensuring mission success.

3. Increased robustness against disturbances and uncertainties

In addition to guaranteeing convergence within a specified time interval, predefined-time stability significantly enhances system robustness against uncertainties and environmental disturbances. In the complex and unpredictable space environment—where solar radiation pressure, atmospheric drag, and mass distribution changes due to fuel consumption are unavoidable—this property is critical for maintaining reliable performance.

4. Efficient use of fuel and resources

By enabling the satellite to achieve the desired orientation quickly and accurately, predefined-time stability reduces the need for unnecessary corrective maneuvers. This decreases the stress imposed on actuators, optimizes propellant consumption, and ultimately extends the satellite's operational lifetime.

Owing to these unique advantages, predefined-time stability has become one of the main research focuses in the contemporary field of spacecraft attitude control. By guaranteeing precise convergence within a specified time interval determined by the designer, this approach provides the predictability required for mission-critical applications—applications in which timing cannot be left to chance. In addition to space systems, the principles of predefined-time control are being increasingly applied in other engineering domains such as robotics, power systems, and automated manufacturing, where reliable performance and robustness against disturbances are of great importance. This expanding range of applications indicates that predefined-time stability is not merely a specialized tool, but rather a versatile framework for designing the next generation of robust control strategies.

Despite these advantages, achieving predefined-time stability in satellite attitude control, particularly in the presence of uncertainties and unknown disturbances, remains challenging. Many existing methods in this field strongly depend on an accurate system model or require knowledge of explicit disturbance bounds—information that, in practice, is often unavailable or unreliable. These limitations have directed researchers' attention toward model-free and data-driven control frameworks—approaches that are designed without relying on an accurate dynamical model and are highly suitable for space systems with unavoidable uncertainties [3].

One common and practically significant approach to enhancing satellite attitude control in the presence of uncertainties is to estimate the "lumped uncertainty function" of the system—the aggregated effect of parametric uncertainties (such as inertia matrix errors), unmodeled dynamics, actuator imperfections, and external disturbance torques—and subsequently design a compensatory input based on this estimate. In the literature, the main research directions for estimating this function can generally be classified into three categories: learning-based intelligent methods, model/observer-based methods, and model-free methods [2]. Intelligent methods such as fuzzy logic and neural networks—including Multilayer Perceptron (MLP), Radial Basis Function (RBF) networks, and neuro-fuzzy hybrid structures—are highly attractive due to their ability to approximate complex nonlinear functions and adapt to time-varying disturbances without requiring an explicit disturbance model. However, their performance is typically sensitive to design choices, such as network architecture, persistent excitation conditions for learning, adaptation gains, and regularization mechanisms. On the other hand, sensitivity to measurement noise, computational constraints, and the difficulty of providing strict transient guarantees (especially exact convergence time guarantees for the estimation error) represent serious challenges for this family of methods, particularly when the learning loop interacts with discontinuous robust components (like sliding mode) or actuator saturation [1].

In contrast, model-based methods such as disturbance observers (DOB) and extended state observers (ESO)—including nonlinear and sliding mode variants—usually offer a more explicit estimation mechanism and a clearer framework for stability analysis, especially when a sufficiently accurate dynamic model is available and observer assumptions (such as matching conditions, boundedness of disturbance derivatives, and appropriate relative degree) are satisfied. Nevertheless, in satellite applications, unavoidable variations in inertia parameters and unmodeled couplings can cause observer performance to remain dependent on model quality. Furthermore, increasing gains to achieve faster convergence may amplify noise and lead to phenomena such as the peaking effect. Many such designs also implicitly assume the existence of explicit bounds for disturbances, which in practice are either unavailable or chosen very conservatively [9]. Under these circumstances, model-free methods such as Time-Delay Estimation (TDE) minimize dependency on an accurate model and reduce the need for known explicit uncertainty bounds by directly reconstructing the lumped uncertainty from measured signals and relying on the short-term continuity of the dynamics [3]. This feature is particularly valuable in satellite attitude control, as orbital disturbances and inertia variations across different mission phases are difficult to parameterize accurately. Although TDE can be sensitive to noise and requires careful selection of delay steps and filtering strategies, it provides a realistic and efficient trade-off in practice: fast, implementable estimation with minimal prior information, and the possibility of "online cancellation" of a major portion of the disturbance. This, in turn, can reduce the required robust gains and mitigate conservatism and chattering. Crucially, while some prior studies in satellite attitude control using TDE have reported excellent results [3], many of the employed controllers only guarantee finite-time stability or offer a settling time that is implicit and scenario-dependent. This creates a clear motivation to move beyond purely finite-time frameworks toward model-free schemes with guaranteed predefined-time stability—where the uncertainty effect is compensated by TDE and the closed-loop response follows a convergence time specified by the designer, a metric that is often the most important performance indicator in fast and time-critical satellite maneuvers.

Among various estimation methods, Time-Delay Estimation is recognized as a simple yet efficient tool that reconstructs unknown dynamics using delayed measurements, eliminating the need for complex observers or heavy learning structures [3]. Accordingly, the integration of model-free control, disturbance estimation, and predefined-time stability represents a highly promising path for developing the next generation of satellite attitude control systems. Such a framework has the capability to provide precise, fast, and robust control under real-world conditions with severe uncertainties, while providing explicit performance guarantees—guarantees that play a key role in advanced and future space missions.

Research Gap

Despite significant advances in predefined-time stability control theory for nonlinear systems, including the attitude dynamics of spacecraft and satellites, fundamental and unresolved gaps remain in the existing literature. First, although predefined-time stability has been investigated using various Lyapunov functions, many of these functions suffer from limited design flexibility and typically rely on a small number of tunable parameters and relatively restrictive assumptions; this makes their practical implementation difficult in the presence of severe uncertainties and time-varying disturbances. Second, in most satellite attitude control designs with guaranteed predefined-time stability that address uncertainty compensation, the estimation of the lumped disturbance function is primarily based on learning-oriented intelligent methods—such as neural networks and fuzzy logic—or model-based methods like disturbance observers. While these approaches are effective, they are either accompanied by the complexities of learning, parameter tuning, and computational load, or they depend on relatively accurate knowledge of the system model and disturbance bounds. To the authors' knowledge, an integrated control framework that simultaneously provides a rigorous proof of predefined-time stability and utilizes a model-free estimation method, such as Time-Delay Estimation (TDE), has not yet been reported. Furthermore, it should be noted that all predefined-time stability Lyapunov functions introduced in the literature to date are based on the boundedness property of the inverse tangent function, and other similar functions, such as the error function ($\mathrm{erf}(x)$), have not been utilized for this purpose.

Contributions of the Paper

In response to the aforementioned gaps, this paper presents a fully integrated, model-free control framework with guaranteed predefined-time stability for satellite attitude control in the presence of uncertainties and external disturbances. First, a novel predefined-time stability Lyapunov function is introduced, which features a more comprehensive parametric structure and provides greater flexibility in shaping the transient behavior and system convergence speed. Unlike existing functions, the proposed function allows for explicit tuning of convergence characteristics while ensuring rigorous and complete proofs of predefined-time stability under practical conditions, including lumped uncertainties and unknown disturbance torques. Second, by moving away from learning-oriented and model-based methods, the proposed controller employs Time-Delay Estimation (TDE) as a model-free mechanism for the online reconstruction of the lumped uncertainty function; thus, the requirement for precise knowledge of the inertia matrix, disturbance bounds, and adaptive learning loops is eliminated. This integration provides, for the first time, a satellite attitude control scheme with predefined-time stability that is truly model-free.

The remainder of this paper is organized as follows. In Section 2, the attitude dynamics of a rigid satellite with uncertainties and subject to external disturbances are investigated using Modified Rodrigues Parameters (MRP). Section 3 is dedicated to presenting the model-free sliding mode controller based on Time-Delay Estimation with guaranteed predefined-time stability. Finally, Section 4 presents the simulation results, performance analysis of the control system, and a comparison with other authoritative studies.

2. Satellite Attitude Dynamics

2-1. Modeling Satellite Attitude Dynamics Using Modified Rodrigues Parameters (MRP)

In the research literature, several methods have been proposed for describing the attitude dynamics and kinematics of satellites, each with its own advantages and limitations. Among the most common of these methods are Euler angles, Euler–Rodrigues parameters (quaternion formulation), Cayley–Klein parameters, and Cayley–Rodrigues parameters, which are used to express the kinematics and dynamics of satellites [1], [4]. The existence of singularity is a common characteristic of all three-dimensional parameterizations; for example, Rodrigues parameters become singular at 180° rotations. The choice of an appropriate parameterization depends on several factors, including the type of spacecraft rotational maneuver, processing requirements, and the degree of physical insight obtained from the attitude representation.

In most control applications, it is desirable to employ a parameterization whose singularity lies at a suitable distance from the origin. The quaternion representation is one of the most common methods for evaluating spacecraft attitude. In this representation, the

kinematic equations are linear with respect to angular velocities and no singularity is introduced for any rotation about the eigenaxis or any algebraic attitude matrix. However, the quaternion representation does not constitute a minimal parameterization, as it describes attitude using four components and requires enforcing the unit-norm constraint on the quaternion [4].

Although the quaternion method offers the advantage of eliminating singularity from the kinematic equations, the use of an additional parameter leads to a non-minimal parameterization. In recent years, Modified Rodrigues Parameters have been widely used in spacecraft attitude control applications, as they enable the representation of rotations up to 360° [4]. MRP provide a minimal three-dimensional parameterization. Nevertheless, this representation is also constrained in maneuvers involving very large angles due to the singularity at the 180° rotation angle. One proposed solution for overcoming this issue is the use of successive rotations with an angle of less than 180° at each step. Although this approach can circumvent the singularity, it may lead to increased control authority requirements, power consumption, and implementation complexity.

The MRP-based dynamical description offers notable advantages, including the ability to represent rotations up to 360° and the possession of a minimal number of parameters [4]:

The simultaneous use of intelligent control methods and chattering-free controllers can significantly reduce the increased power consumption resulting from this representation. Furthermore, in the design of satellite attitude observers and estimators, the use of Modified Rodrigues Parameters is often preferred over the quaternion method, as it not only reduces the computational load but also simplifies the mathematical calculations associated with controller design. Accordingly, in the present study, this modeling framework is employed to describe the attitude kinematics and dynamics of the satellite.

The modeling of attitude dynamics using Modified Rodrigues Parameters and its complete explanation can be studied in references [4], which are presented here in a summarized form. Let $\sigma \in \mathbb{R}^3$denote the Modified Rodrigues Parameters, defined by the following relationship:

$$\sigma = [\sigma_1 \ \sigma_2 \ \sigma_3]^T = \hat{e} \tan\frac{\theta}{4} \tag{1}$$

where $\hat{e} = [e_1 \ e_2 \ e_3]$ are the unit vectors of the Euler axis rotation and θ denotes the rotation about the principal axis. The attitude kinematics based on the Modified Rodrigues Parameters can be expressed as:

$$\dot{\sigma} = \Gamma(\sigma)\, \omega \tag{2}$$

where $\omega$is the angular velocity expressed in the body frame $[x\ y\ z]$relative to the inertial frame $[X\ Y\ Z]$, and the function $\Gamma(\sigma)$is expressed as:

$$\Gamma(\sigma) = \frac{1}{4}[(1 - \sigma^T\sigma)\, I_{3\times3} + 2S^*(\sigma) + 2\sigma\sigma^T] \tag{3}$$

where $I_{3\times3}$denotes the identity matrix and $S^*(\sigma)$is the skew-symmetric matrix of the Modified Rodrigues Parameters, defined as:

$$S^*(\sigma) = \begin{bmatrix} 0 & -\sigma_3 & \sigma_2 \\ \sigma_3 & 0 & -\sigma_1 \\ -\sigma_2 & \sigma_1 & 0 \end{bmatrix} \tag{4}$$

If the control input vector is denoted by $u(t) \in \mathbb{R}^3$and the external disturbances acting on the system by $d(t) \in \mathbb{R}^3$, then the satellite system dynamics can be expressed as:

$$J\dot{\omega} = -S^*(\omega)J\omega + u(t) + d(t) \tag{5}$$

where Jdenotes the system inertia matrix and $S^*(\omega)$is the skew-symmetric matrix of the angular velocities. By combining the above equations, the Euler–Lagrange form of the satellite dynamic and kinematic equations can be written as a single unified equation:

$$M(\sigma)\ddot{\sigma} + C(\sigma, \dot{\sigma})\dot{\sigma} = \tau + \tau_{ext} \tag{6}$$

This equation is analogous to the Euler–Lagrange form of the dynamic equations in robotic systems. The advantage of this modeling approach lies in the unification of the system kinematics and dynamics. Therefore, there is no need to design separate controllers for attitude control at the kinematic and dynamic levels, which simplifies the controller design process. From a computational standpoint,

this also entails a reduction in the amount of mathematical calculations and processing costs. The terms appearing in the above equation are computed as follows:

$$M(\sigma) = \Gamma(\sigma)^{-T} J\, \Gamma(\sigma)^{-1} \tag{7a}$$

$$C(\sigma, \dot{\sigma}) = -\Gamma(\sigma)^{-T} J\, \Gamma(\sigma)^{-1} \dot{\Gamma}(\sigma) \Gamma(\sigma)^{-1} - \Gamma(\sigma)^{-T} S^*(J\omega)\, \Gamma(\sigma)^{-1} \tag{7b}$$

$$\tau = \Gamma(\sigma)^{-T} u(t) \tag{7c}$$

$$\tau_{ext} = \Gamma(\sigma)^{-T} d(t) \tag{7d}$$

In the design of nonlinear control systems, the "affine" form of the equations is typically required, which expresses the system dynamics as second-order differential equations in the following form:

$$\begin{cases} \dot{x}_1 = x_2 \\ \dot{x}_2 = f(x) + g(x)u + d \\ y = x \end{cases} \tag{8}$$

For the satellite dynamic equations obtained using Modified Rodrigues Parameters, by considering $x_1 = \sigma$and $x_2 = \dot{\sigma}$, the dynamic equations can be written in affine form so that the general form of the equations matches the above equation, where the functions $f(x)$, $g(x)$, and $d$are computed as:

$$\begin{cases} f(x) = M^{-1}(\sigma)\, C(\sigma, \dot{\sigma})\, \dot{\sigma} \in \mathbb{R}^3 \\ g(x) = M^{-1}(\sigma)\, \Gamma(\sigma)^{-T} \in \mathbb{R}^3 \\ d = M^{-1}(\sigma)\, \Gamma(\sigma)^{-T}\, d(t) \in \mathbb{R}^3 \end{cases} \tag{9}$$

2-2. Attitude Error Dynamics Using Modified Rodrigues Parameters

The dynamic model presented in the previous section examines system control within the framework of a tracking problem. By defining the attitude error dynamics, the problem can be transformed into an attitude regulation problem. To derive the equations governing the attitude error dynamics, if we assume $\sigma_d \in \mathbb{R}^3$to be the desired system attitude and $\omega_d \in \mathbb{R}^3$the desired angular velocities, then the system attitude error with respect to the desired inputs can be expressed as:

$$\begin{cases} \sigma_e = \dfrac{(1 - \sigma_d^T \sigma_d)\sigma - (1 - \sigma^T \sigma)\sigma_d + 2S'(\sigma)\sigma_d}{1 + \sigma^T \sigma\, \sigma_d^T \sigma_d + 2\sigma_d^T \sigma} \\ \omega_e = \omega - Z(\sigma_e)\, \omega_d \end{cases} \tag{10}$$

where the function $Z(\sigma_e)$is defined as:

$$Z(\sigma_e) = Z(\sigma)\, Z(\sigma_d) \tag{11a}$$

$$Z(\sigma) = I_{3\times3} - \frac{4(1 - \sigma^T \sigma)}{(1 + \sigma^T \sigma)^2} S^*(\sigma) + \frac{8S^*(\sigma)}{(1 + \sigma^T \sigma)} S^*(\sigma) \tag{11b}$$

$$Z(\sigma_d) = I_{3\times3} - \frac{4(1 - \sigma_d^T \sigma_d)}{(1 + \sigma_d^T \sigma_d)^2} S^*(\sigma_d) + \frac{8S^*(\sigma_d)}{(1 + \sigma_d^T \sigma_d)} S^*(\sigma_d) \tag{11c}$$

The attitude error kinematics can now be expressed based on $\sigma_e$and $\omega_e$as:

$$\dot{\sigma}_e = G(\sigma_e)\, \omega_e \tag{12}$$

Similarly, the attitude error dynamics equation can be written as:

$$J\dot{\omega}_e = -S^*(\omega_e + Z(\sigma_e)\omega_d)\, J(\omega_e + Z(\sigma_e)\omega_d) - J\dot{Z}(\sigma_e)\omega_d - JZ(\sigma_e)\dot{\omega}_d + u(t) + d(t) \tag{13}$$

By combining the kinematic and dynamic error equations, the Lagrangian form of the attitude error dynamics can be expressed as:

$$M(\sigma_e)\ddot{\sigma}_e + C(\sigma_e, \dot{\sigma}_e)\dot{\sigma}_e + G(\sigma_e) = \tau + \tau_{ext} \tag{14}$$

The various components of the above equation are:

$$M(\sigma_e) = \Gamma(\sigma_e)^{-T} J\, \Gamma(\sigma_e)^{-1} \tag{15a}$$

$$C(\sigma_e,\dot{\sigma}_e) = \Gamma(\sigma_e)^{-T} J\,\dot{\Gamma}(\sigma_e)^{-1} - \Gamma(\sigma_e)^{-T} S^*(J\omega_e)\,\Gamma(\sigma_e)^{-1} - \Gamma(\sigma_e)^{-T}(S^*(JZ(\sigma_e)\omega_d))\Gamma(\sigma_e)^{-1} + \Gamma(\sigma_e)^{-T}(JS^*(Z(\sigma_e)\omega_d) + S^*(Z(\sigma_e)\omega_d)J)\Gamma(\sigma_e)^{-1} \quad (15b)$$

$$G(\sigma_e) = \Gamma(\sigma_e)^{-T}(S^*(Z(\sigma_e)\omega_d)\,JZ(\sigma_e)\omega_d) + JZ(\sigma_e)\dot{\omega}_d \quad (15c)$$

$$\tau = \Gamma(\sigma_e)^{-T} u(t) \quad (15d)$$

$$\tau_{ext} = \Gamma(\sigma_e)^{-T} d(t) \quad (15e)$$

Now, to obtain the state-space form of the above equations for use in the control system design, by considering the state variables $x_1 = \sigma_e$ and $x_2 = \dot{\sigma}_e$, the attitude error dynamics can be expressed as:

$$\begin{cases} \dot{x}_1 = x_2 \\ \dot{x}_2 = f(x) + g(x)u + d \\ y = x = [x_1, x_2] = [\sigma_e, \dot{\sigma}_e] \end{cases} \quad (16)$$

where the dynamic functions are $f(x) = M^{-1}(\sigma_e)\,C(\sigma_e,\dot{\sigma}_e)\,\dot{\sigma}_e \in \mathbb{R}^3$, $g(x) = M^{-1}(\sigma_e)\,\Gamma(\sigma_e)^{-T} \in \mathbb{R}^3$, and $d = (M^{-1}(\sigma_e)\,\Gamma(\sigma_e)^{-T} d(t) - M^{-1}(\sigma_e)\,\Gamma) \in \mathbb{R}^3$. Since the function $d$represents the external disturbances acting on the system and takes bounded values, it is assumed to have an upper bound expressed as $|\,d\,| \leq \delta_d$. Moreover, the parametric uncertainties of the system—such as uncertainty in the system's moments of inertia—induce bounded uncertainties in the functions $f(x)$and $g(x)$, which can be described in general as:

$$\begin{cases} f(x) = f_0(x) + \Delta f(x), & |\,\Delta f(x)\,| \leq \delta_f \\ g(x) = g_0(x) + \Delta g(x), & |\,\Delta g(x)\,| \leq \delta_g \end{cases} \quad (17)$$

Furthermore, considering the power generation limits of the actuators and their saturation, a bound for the control inputs can also be defined as $|\,u\,| \leq \delta_u$. Now, taking into account the defined bounds for the uncertainties, external disturbances, and control inputs, equation (16) can be rewritten as:

$$\begin{cases} \ddot{x} = f_0(x) + g_0(x)u + D \;\rightarrow\; \ddot{\sigma}_e = f_0(\sigma_e,\dot{\sigma}_e) + g_0(\sigma_e,\dot{\sigma}_e)u + D(t) \\ y = x \end{cases} \quad (18)$$

where the function $D(t) = \Delta f(x) + \Delta g(x)u + d$represents the sum of the parametric uncertainties and external disturbances acting on the system. For this function, an upper bound can be defined based on the bounds established for the uncertainties and external disturbances as:

$$\begin{cases} |\,D\,| \leq |\,\Delta f + \Delta g\,\delta_u + \delta_d\,| \leq |\,\delta_f + \delta_g\delta_u + \delta_d\,| \leq \Delta_D \\ |\,\dot{D}(x,u,t)\,| \leq \overline{\Delta}_D \end{cases} \quad (19)$$

The uncertainties considered in the dynamic functions (Δf and Δg) arise from the presence of uncertainty in the moments of inertia. To better understand the effect of the uncertainty in the satellite's moments of inertia on the system dynamic equations, we first rewrite the satellite attitude dynamics equation stated in equation (5) as:

$$\dot{\omega} = J^{-1}(-S^*(\omega)J\omega + u(t) + d(t)) \quad (20)$$

If we assume that the inertia moment matrix contains an uncertainty of the form δJ, then the satellite's moment of inertia can be written as $J = J_0 + \delta J$. Considering the uncertainty in the moment of inertia and using the matrix inverse sum theorem, the inverse of the inertia moment matrix in the presence of uncertainties can be computed as [2]:

$$\begin{cases} J^{-1} = (J_0 + \delta J)^{-1} = J_0^{-1} + \delta\hat{J} \\ \delta\hat{J} = -J_0^{-1}\,\delta J\,(I_{3\times3} + J_0^{-1}\delta J)^{-1} J_0^{-1} \end{cases} \quad (21)$$

Uncertainty in the calculation of the satellite's moments of inertia typically arises for two reasons: uncertainty resulting from modeling in the satellite system's mechanical design software, and uncertainty caused by errors in computing the satellite's principal rotation axis relative to its body. The modeling of each of these uncertainties can be performed as follows in order to obtain a more accurate form of the uncertainty description stated in equation (21) and to use it in the formation of the dynamic function uncertainties [1]:

$$\begin{cases} \delta J \triangleq \Delta J_1 + \Delta J_2 \\ \Delta J_1 \triangleq \begin{bmatrix} \delta_1 J_1 & 0 & 0 \\ 0 & \delta_2 J_2 & 0 \\ 0 & 0 & \delta_3 J_3 \end{bmatrix} \rightarrow \ \delta_1, \delta_2, \delta_3 \in \left[-, \bar{\delta}_{J1} + \bar{\delta}_{J1}\right] \\ \Delta J_2 \triangleq \left(1 + \bar{\delta}_{J1}\right) \max(J_1, J_2, J_3) \begin{bmatrix} \delta_{11} & \delta_{12} & \delta_{13} \\ \delta_{12} & \delta_{22} & \delta_{23} \\ \delta_{13} & \delta_{23} & \delta_{33} \end{bmatrix} \rightarrow \ \delta_{ij} \in \left[-, \bar{\delta}_{J2} + \bar{\delta}_{J2}\right], \ \ i, j = 1,2,3 \end{cases} \tag{22}$$

where δ_{ij}can be chosen as random numbers within a bounded interval.

It should be noted that the importance of modeling the moment of inertia uncertainty lies in ensuring the robustness of the controller, and by considering this aspect, a better assessment of the robustness of the satellite control system in the presence of uncertainties and external disturbances acting on the system can be achieved.

3. Model-Free Sliding Mode Controller Design with Predefined-Time Stability Based on Time-Delay Estimation

3-1. Overview of Stability Concepts in Nonlinear Systems

This section examines the fundamental definitions of finite-time stability for non-autonomous dynamic systems.

Consider the nonlinear non-autonomous dynamic system $\dot{x} = f(x,t)$ [42], [43], [44], [45], where the function $f: \mathbb{R}^n \times [0,\infty) \rightarrow \mathbb{R}^n$is piecewise continuous with respect to the time variable and satisfies local Lipschitz continuity with respect to the state variable. Consequently, the existence and uniqueness of the system response over a specified time interval are guaranteed. The point $x = 0$is considered as the system equilibrium point, whose stability is defined as follows:

Lyapunov Stability: The system $\dot{x} = f(x,t)$is called Lyapunov stable if, for every small positive value $\varepsilon > 0$, there exists a value $\delta(\varepsilon) > 0$such that if the system's initial condition satisfies $\mid x(0) \mid \leq \delta(\varepsilon)$, the system trajectory remains bounded for all times. In simpler terms, for all $t \geq 0$, we have $\mid \phi(x,(0)t) \mid \leq \varepsilon$. This type of stability is simple and requires minimal conditions, keeping the system trajectory within a safe bound. However, it provides no specified convergence time and is insufficient for time-critical, sensitive missions.

Asymptotic Stability: The dynamic system $\dot{x} = f(x,t)$is asymptotically stable if it is initially Lyapunov stable and, moreover, the system trajectories gradually converge to the equilibrium point over time: $\lim_{t\rightarrow+\infty} \mid \phi(x,(0)t) \mid \rightarrow 0$. This type of stability guarantees that the system naturally returns to the origin and is robust against initial perturbations; however, the convergence rate is not controllable and may be unreliable for real systems such as spacecraft.

Finite-Time Stability: The system $\dot{x} = f(x,t)$is finite-time stable if, in addition to satisfying the Lyapunov stability conditions, its trajectories reach the equilibrium point within a finite time interval. Mathematically, there exists a settling-time function $T\big(x(0)\big)$such that for $t \geq T\big(x(0)\big)$, $\mid \phi(x,(0)t) \mid = 0$. This type of stability is faster than the asymptotic case and guarantees that the error reaches zero in a finite time; however, the convergence time depends on the initial conditions, making the design more complex.

Fixed-Time Stability: The system $\dot{x} = f(x,t)$is fixed-time stable if, in addition to satisfying the finite-time stability conditions, the time to reach equilibrium is bounded and uniform for all initial conditions. In other words, there exists a maximum settling time T_{max}such that: $\sup_{x_0 \in \mathbb{R}^n} T(x_0) \leq T_{max}$. This property endows the system with uniform stability across all initial conditions, making it suitable for real systems requiring guaranteed performance speed. However, the controller design is more complex and may require high-power nonlinear controllers and precise parameter tuning.

Predefined-Time Stability: The dynamic system $\dot{x} = f(x,t)$is predefined-time stable if, in addition to satisfying fixed-time stability, the maximum time to reach equilibrium can be specified explicitly and prior to system design. This property is realized in control by introducing a tunable positive parameter T_c, such that: $\sup_{x_0 \in \mathbb{R}^n} T(x_0) \leq T_c$. This feature enables precise tuning of the system response according to mission requirements and is particularly useful for critical scenarios such as coordinated satellite maneuvers. The mathematical analyses and controller design in this case are more complex and require specialized control functions to achieve the predefined convergence time.

Therefore, each type of stability has its own advantages and limitations, and the appropriate selection for the controller design of satellite systems directly affects the performance of the space mission. Lyapunov stability keeps the system trajectory within a safe

bound, asymptotic stability contributes to the natural return to equilibrium, finite-time and fixed-time stability enable prediction of the convergence rate, and predefined-time stability offers the greatest control and flexibility for executing critical missions.

3-2. Lyapunov Functions Used in Predefined-Time Convergence Controllers

Lyapunov theory is one of the fundamental tools in the stability analysis of dynamic systems. The core idea of this theory is the use of a positive and differentiable function, called the Lyapunov function, which describes the system behavior around the equilibrium point. If such a function can be found that is always positive and whose time derivative is negative, the stability of the system's equilibrium point can be guaranteed. In the design of controllers with predefined-time convergence, Lyapunov functions serve as a key tool for guaranteeing system convergence within a specified and tunable time interval. These functions enable the design of control laws that render the convergence rate tunable and drive the system response to the equilibrium point independently of the initial conditions.

In recent years, the development of control methods with predefined-time convergence has become one of the important topics in the design of complex dynamic systems. In this field, controllers have been designed that guarantee system performance within a specified and tunable time interval. Table (1) presents the various Lyapunov functions that have been employed in the design of such controllers, each offering its own specific features and advantages in ensuring system stability and convergence speed.

Table (1): Lyapunov functions used in the design of controllers with predefined-time convergence

Ref.	Functions
[27]	$\dot{V} \le \frac{-\pi}{\alpha T_c}\left(V^{1-\alpha/2} + V^{1+\alpha/2}\right)$
[40]	$\dot{V} \le \frac{-\pi}{\alpha T_c\sqrt{\rho\delta}}\left(\rho V^{1-\alpha/2} + \delta V^{1+\alpha/2}\right)$
[24], [25]	$\dot{V} \le -\frac{\pi}{\eta\mu T_c}\left[V^{1-\frac{\eta}{2}} + \mu^2 V^{1+\frac{\eta}{2}}\right]$
[30], [31]	$\dot{V} \le -\frac{1}{\eta T_c}\exp[V^{\eta}]V^{1-\eta}, \forall x \neq 0$
[43]	$\dot{V} \le -\frac{\alpha^{\frac{\beta q-1}{\eta}}\Gamma\left(\frac{1-\beta q}{\eta}\right)}{\eta T_c} exp(\alpha V^{\eta})V^{\beta q}$

The functions presented in the above table are constructed based on integrals whose closed-form solution involves the inverse tangent function. Since the inverse tangent function is bounded, these functions are also bounded, and they are therefore referred to as "predefined-time functions." However, it should be emphasized that this approach is not limited solely to integrals with inverse tangent responses; rather, any integral whose output is a bounded function can be employed within this same framework. Accordingly, a new function is introduced in the following section, which will be utilized throughout the remainder of this study.

3-3. Derivation of the Proposed Lyapunov Function Relationships

In this section, the procedure for deriving the final inequality required to design a controller with a predefined convergence time, based on the classical integration method, is described. The primary objective of this analysis is to guarantee the convergence of the system states within a specified and finite time interval, namely $T_c > 0$. To this end, the derivation process begins by considering the following differential inequality:

$$\dot{x} \le -\frac{\mu_1}{T_c} e^{\left(x^2+2\beta x\right)} \tag{23}$$

where $x(t)$is an auxiliary variable associated with the Lyapunov function, $T_c$is the predefined convergence time, $\beta$is a positive constant coefficient, and $\mu_1 = \frac{\sqrt{\pi}}{2}\, e^{\beta^2}(1 - erf(\beta))$. By employing the standard integration relationship, we have:

$$\int_0^{\infty} e^{-(x^2+2\beta x)}dx = \frac{\sqrt{\pi}}{2}\, e^{\beta^2}(1 - erf(\beta)) \tag{24}$$

Now, by rewriting inequality (23) and performing the integration for the maximum value of the integral over the interval $[0, \infty)$, the following relationship is obtained:

$$\int_0^{\infty} e^{-(x^2+2\beta x)} dx \leq -\frac{\mu_1}{T_c} \int_0^{T^*} d\,t \tag{25}$$

By computing the values of the integrals, the following result is obtained:

$$\frac{\mu_1}{T_c}(T^*) \leq \mu_1 \;\Rightarrow\; T^* \leq T_c \tag{26}$$

This result demonstrates that the auxiliary variable $x(t)$converges to zero from its initial value within a time less than or equal to T_c. In order to generalize this result to the Lyapunov function $V(t)$, the transformation $x = V^{\eta/2}$is considered, where $0 < \eta < 1$. By differentiation, the following relationship is obtained:

$$dx = \frac{\eta}{2} V^{\eta/2-1}\, dV \;\Rightarrow\; \frac{dx}{dt} = \frac{\eta}{2V^{1-\eta/2}} \frac{dV}{dt} \tag{27}$$

By substituting this transformation into inequality (23), the desired inequality is transferred to the Lyapunov function and expressed as follows:

$$\frac{\eta}{2V^{1-\eta/2}} \dot{V} \leq -\frac{\mu_1}{T_c} e^{\left(V^{\eta}+2\beta V^{\eta/2}\right)} \tag{28}$$

By simplifying the above relationship, the Lyapunov inequality is rewritten as:

$$\dot{V} \leq -\frac{2\mu_2}{\eta T_c} V^{1-\eta/2} e^{\left(V^{\eta}+2\beta V^{\eta/2}\right)} \tag{29}$$

Finally, by substituting the value of $\mu_1$into inequality (29), the final Lyapunov inequality for the system with predefined convergence time is obtained as:

$$\dot{V} \leq -\frac{\sqrt{\pi}}{\eta T_c}\left[\, e^{\beta^2}(1 - erf(\beta))\right] V^{1-\eta/2} e^{\left(V^{\eta}+2\beta V^{\eta/2}\right)} \tag{30}$$

This inequality guarantees that the Lyapunov function V, independently of the initial conditions, converges to zero within a time less than or equal to T_c.

3-4. Proposed Controller Design

To design the control system, we first consider the second-order nonlinear satellite attitude dynamics given in equations (16) and (17). In the aforementioned equation, $D(x,t)$represents the lumped uncertainty of the system and is bounded, i.e., $| D | < \Delta$. In the present study, the time-delay estimation (TDE) method is employed to compensate for the unknown disturbance. The main assumption of this method is that the disturbance does not undergo significant variation over a small time interval L. Therefore,

$$\widehat{D}(t) \cong D(t - L) \tag{31}$$

or equivalently,

$$\widehat{D}(x,t) = \widehat{D}(x(t-L), t-L) \tag{32}$$

Using the system dynamics, the disturbance estimate is constructed as follows:

$$\widehat{D} = \dot{x}_2(t-L) - f(x(t-L), t-L) - g(x(t-L), t-L)u(t-L) \tag{33}$$

The disturbance estimation error is expressed as:

$$\widetilde{D} = D - \widehat{D} = D - D(x(t-L), t-L) \cong D - D(t-L) \tag{34}$$

Assuming Lipschitz continuity for the disturbance, we have:

$$\widetilde{D} \leq \rho \mid t - (t-L) \mid \cong \rho L \cong \epsilon \tag{35}$$

which implies that $\widetilde{D} \leq \epsilon$. Therefore, by selecting sufficiently small values of L, the disturbance estimation error can be made arbitrarily small.

Since

$$\dot{x}_2(t-l) = \ddot{x}_1(t-l) \tag{36}$$

the second derivative of the state can be expressed using the finite-difference approximation as:

$$\begin{cases} \ddot{x}_1(t-L) = \dfrac{x_1(t) - 2x_1(t-L) + x_1(t-2L)}{L^2}, & t \geq T \\ \ddot{x}_1(t-L) = 0, & t < T \end{cases} \tag{37}$$

where the condition $T \geq 2L$holds. This condition ensures the availability of delayed data for estimation. To guarantee predefined-time stability independent of the initial conditions, consider a candidate Lyapunov function whose rate of change satisfies:

$$\dot{V} \leq -\frac{2\mu}{\eta T_c} V^{1-\eta/2}\, e^{\left(V^{\eta} + 2\beta V^{\eta/2}\right)} \tag{38}$$

where $\mu = \frac{\sqrt{\pi}}{2}\, e^{\beta^2}(1 - erf(\beta))$. The above inequality guarantees predefined-time convergence through the nonlinear exponential term in V.

By introducing the tracking error as $e = x - x_d \cong \sigma_e$, the sliding surface is defined as:

$$S = \dot{\sigma}_e + \lambda \sigma_e \tag{39}$$

The time derivative of the sliding surface is:

$$\dot{S} = \ddot{\sigma}_e + \lambda \dot{\sigma}_e \tag{40}$$

To enforce predefined-time convergence of the sliding surface, we require:

$$\dot{S} \leq -\frac{2\mu}{\eta T_c} S^{1-\eta/2}\, e^{\left(s^{\eta} + 2\beta s^{\eta/2}\right)} \tag{41}$$

Substituting the system dynamics into the above inequality yields:

$$f + gu + D + \lambda \dot{\sigma}_e \leq -\frac{2\mu}{\eta T_c} S^{1-\eta/2}\, e^{\left(s^{\eta} + 2\beta s^{\eta/2}\right)} \tag{42}$$

and therefore,

$$gu \leq -[f + D + \lambda\dot{\sigma}_e + \frac{2\mu}{\eta T_c} S^{1-\eta/2}\, e^{\left(s^{\eta} + 2\beta V^{S/2}\right)}\ ] \tag{43}$$

Hence, the control input is obtained as:

$$u = g^{-1}\left[f + \lambda\dot{\sigma}_e + \frac{2\mu}{\eta T_c} S^{1-\eta/2}\, e^{\left(s^{\eta} + 2\beta s^{\eta/2}\right)} - \Delta\,\mathrm{sign}(S)\right] \tag{44}$$

Also, the control input considering time-delay estimation is given by:

$$U^{*}_{TDE} = \dot{g}^{-1}\left[f + \lambda\dot{\sigma}_e + \frac{2\mu}{\eta T_c} S^{1-\eta/2}\, e^{\left(s^{\eta} + 2\beta s^{\eta/2}\right)} - \widehat{D}\right] \tag{45}$$

By substituting the control input into the sliding dynamics, we obtain:

$$\dot{S} = -\frac{2\mu}{\eta T_c} S^{1-\eta/2} e^{\left(s^{\eta} + 2\beta s^{\eta/2}\right)} + D - \Delta\,\mathrm{sign}(S) \tag{46}$$

Since $D \leq \mid D \mid \leq \Delta$, we have:

$$D - \Delta\,\mathrm{sign}(S) \leq \mid D \mid -\Delta\,\mathrm{sign}(S) \leq \Delta - \Delta\,\mathrm{sign}(S) \leq \Delta\big(1 - \mathrm{sign}(S)\big) \tag{47}$$

Given that $-1 \leq \mathrm{sign}(S) \leq 1$, one can write

$$D - \Delta\,\mathrm{sign}(S) \leq 2\Delta = \rho \tag{48}$$

Therefore,

$$\dot{S} \leq -\frac{2\mu}{\eta T_c} S^{1-\eta/2}\, e^{\left(s^{\eta} + 2\beta s^{\eta/2}\right)} + \rho \tag{49}$$

which, in the presence of bounded disturbances, represents operational predefined-time stability. If the control input containing the time-delay estimation term in equation (45) is applied to equation (46), the sliding dynamics become:

$$\dot{S} = -\frac{2\mu}{\eta T_c} S^{1-\eta/2}\, e^{\left(s^{\eta} + 2\beta s^{\eta/2}\right)} + D - \widehat{D} = -\frac{2\mu}{\eta T_c} S^{1-\eta/2}\, e^{\left(s^{\eta} + 2\beta s^{\eta/2}\right)} + \widetilde{D} \tag{50}$$

Given that $\widetilde{D} \leq \epsilon$, we can write:

$$\dot{S} \leq -\frac{2\mu}{\eta T_c} S^{1-\eta/2} e^{\left(s^{\eta} + 2\beta s^{\eta/2}\right)} + \epsilon \tag{51}$$

To examine stability, choose the Lyapunov function as:

$$V = \frac{1}{2} S^2 \tag{52}$$

where $S^2 = 2V$ and consequently $S = \sqrt{2V}$. Therefore, the rate of change of the Lyapunov function is:

$$\dot{V} = S\dot{S} \leq S\left(-\frac{2\mu}{\eta T_c} S^{1-\eta/2} e^{\left(s^{\eta}+2\beta s^{\eta/2}\right)} + \rho\right) \tag{53}$$

which gives

$$\dot{V} \leq -\frac{2\mu}{\eta T_c} S^{2-\eta/2}\, e^{\left(s^{\eta}+2\beta s^{\eta/2}\right)} + \rho S \tag{54}$$

By substituting $S = \sqrt{2V}$, we obtain

$$\dot{V} \leq -\frac{2\mu}{\eta T_c} (2V)^{1-\eta/4} e^{\left((2V)^{\eta}+2\beta(2V)^{\eta/2}\right)} + \epsilon \tag{55}$$

Integrating both sides of the above inequality yields:

$$\int_0^{\infty} \frac{dV}{(2V)^{1-\eta/4} e^{\left((2V)^{\eta}+2\beta(2V)^{\eta/2}\right)}} \leq -\frac{2\mu}{\eta T_c} \int_0^{T^*} d\,t \tag{56}$$

By substituting $x = (2V)^{\eta/4}$, and $\frac{dV}{(2V)^{1-\eta/4}} = \frac{2}{\eta} dx$ we can write:

$$\frac{2}{\eta} \int_0^{\infty} e^{-\left(x^2+2\beta x\right)}\, dx \leq -\frac{2\mu}{\eta T_c} \int_0^{T^*} d\,t \tag{57}$$

Since

$$\int_0^{\infty} e^{-\left(x^2+2\beta x\right)}\, dx = \mu \tag{58}$$

it follows that $\frac{2\mu}{\eta T_c} \leq \frac{2}{\eta}\mu \Longrightarrow T^* \leq T_c$, which indicates predefined-time convergence independent of the initial conditions.

Finally, to prove predefined-time stability in the practical case, we have:

$$\begin{gathered} \dot{V} \leq -\frac{2\mu}{\eta T_c} V^{1-\eta/2} e^{\left(V^{\eta}+2\beta V^{\eta/2}\right)} + \delta \\ \Rightarrow\ \dot{V} \leq -\frac{\mu}{\eta T_c} V^{1-\eta/2} e^{\left(V^{\eta}+2\beta V^{\eta/2}\right)} + \delta - \frac{\mu}{\eta T_c} V^{1-\eta/2} e^{\left(V^{\eta}+2\beta V^{\eta/2}\right)} \end{gathered} \tag{59}$$

Thus, in order to satisfy the predefined-time stability condition, the following inequality must hold:

$$\delta - \frac{\mu}{\eta T_c} V^{1-\eta/2} e^{\left(V^{\eta}+2\beta V^{\eta/2}\right)} > 0 \Rightarrow V^{1-\eta/2} e^{\left(V^{\eta}+2\beta V^{\eta/2}\right)} < \frac{\delta \eta T_c}{\mu} \tag{60}$$

and hence,

$$\left\{V:\, V^{1-\eta/2} e^{\left(V^{\eta}+2\beta V^{\eta/2}\right)} < \frac{\delta \eta T_c}{\mu}\right\} \tag{61}$$

By integrating similarly to the previous case, we obtain:

$$\int_0^{\infty} e^{-\left(V^{\eta}+2\beta V^{\eta/2}\right)} \frac{dv}{V^{1-\eta/2}} \leq -\frac{\mu}{\eta T_c}\int_0^{T^*} d\,t \tag{62}$$

Let $V^{\eta/2} = x$, then

$$\frac{\eta}{2}\frac{dV}{V^{1-\eta/2}} = dx \;\Rightarrow\; \frac{dV}{V^{1-\eta/2}} = \frac{2}{\eta}dx \tag{63}$$

Therefore,

$$\frac{2}{\eta}\int_0^{\infty} e^{-\left(V^{\eta}+2\beta V^{\eta/2}\right)}\, dx \leq -\frac{\mu}{\eta\tau_c}\int_0^{T^*} d\,t \;\Rightarrow\; T^* \leq 2T_c \tag{64}$$

Which indicates operational predefined-time stability for the closed-loop system.

Remark 1. In conventional time-delay estimation (TDE) schemes, the delayed acceleration vector is typically approximated using classical second-order finite-difference methods, such as Eq. (37). Although computationally straightforward, numerical differentiation exhibits severe drawbacks in real-world implementations. Specifically, dividing by L^2 inherently acts as a high-pass filter, resulting in substantial noise amplification, degradation of estimation accuracy, and severe chattering in the control input. To circumvent this issue while guaranteeing robust estimation, a Uniform Robust Exact Differentiator (URED) [46] is adopted in this study to reconstruct the required state derivatives.

Unlike standard finite-difference formulas and conventional Levant differentiators whose convergence times grow unboundedly with the initial estimation error, the URED incorporates high-degree correction terms into the sliding-mode manifold. Consequently, it guarantees exact derivative estimation in finite time, exhibits strong robustness against bounded measurement disturbances/noise, and ensures a uniform convergence time that is strictly bounded by a constant independent of initial conditions. This property is crucial for fast transient dynamics and ensures chattering-free and high-precision tracking control.

To reconstruct the time derivatives of the measured signal $x_1(t)$ without numerical differentiation, we employ the URED [46]. The URED provides uniform finite-time convergence, where the convergence time is independent of initial conditions. Given the signal $f(t) = f_0(t) + v(t)$ with a bounded second derivative $\left|\ddot{f}_0(t)\right| \leq L$, the URED is governed by the following system:

$$\dot{z}_0 = -k_1\phi_1(\sigma_0) + z_1, \qquad \dot{z}_1 = -k_2\phi_2(\sigma_0) \tag{65}$$

where z_0 and z_1 are the estimates of $f_0(t)$ and $\dot{f}_0(t)$, respectively. The correction terms φ_1 and φ_2 are defined as:

$$\begin{aligned}\phi_1(\sigma_0) &= |\sigma_0|^{\frac{1}{2}} sign(\sigma_0) + \mu|\sigma_0|^{\frac{3}{2}} sign(\sigma_0),\\ \phi_2(\sigma_0) &= \frac{1}{2}sign(\sigma_0) + 2\mu\sigma_0 + \frac{3}{2}\mu^2|\sigma_0|^2 sign(\sigma_0)\end{aligned} \tag{66}$$

Here, $\sigma_0 = z_0 - f(t)$ denotes the estimation error, $\mu > 0$ is a positive design parameter that enables uniform convergence, and k_1, k_2 are the observer gains. The observer is stable and convergent if the gains (k_1, k_2) satisfy the following condition derived from LMI constraints:

$$\begin{aligned}\mathcal{K} = \{(k_1,k_2) \in \mathbb{R}^2 \mid 0 < k_1 \leq 2\sqrt{L}, k_2 > \frac{k_1^2}{4} + \frac{4L^2}{k_1^2}\Big\}\\ \cup \left\{(k_1,k_2) \in \mathbb{R}^2 \mid k_1 > 2\sqrt{L}, k_2 > 2L\right\}\end{aligned} \tag{67}$$

For numerical implementation, parameters such as $L = 2.5, k_1 = 3.46, k_2 = 6$, and $\mu = 1$ are typical choices that ensure robust derivative estimation.

Remark 2 (Cascaded Derivative Estimation): To accurately obtain both the first and second time derivatives of the attitude tracking error ($\dot{\sigma}_e$ and $\ddot{\sigma}_e$) from noisy measurements without relying on finite-difference approximations, a two-stage cascaded URED configuration is implemented. The first stage takes $\sigma_e(t)$ as input and reconstructs the clean velocity $\hat{\dot{\sigma}}_e(t) = z_{1,1}(t)$. Subsequently, the second stage takes $z_{1,1}(t)$ as its input and estimates the acceleration $\hat{\ddot{\sigma}}_e(t) = z_{2,1}(t)$. Thanks to the uniform finite-time convergence of each stage, the total convergence time of the cascaded differentiator is bounded by the sum of the two settling times ($T_{\text{total}} \leq T_1 + T_2$), guaranteeing rapid, chattering-free, and exact second-order derivative reconstruction.

4. Simulation Results

In this section, the simulation results of the proposed control scheme are presented. To validate the obtained results and to conduct a comprehensive and fair comparison, three other Lyapunov functions previously used in reputable prior studies were also simulated. The functions employed are listed in Table (2).

Table (2): Lyapunov Functions Used in the Design of Controllers with Predefined-Time Convergence

Case	Function	Ref.
Case A	$\dot{V} \leq -\frac{\sqrt{\pi}}{\eta T_c}\left[e^{\beta^2}(1 - erf(\beta))\right] V^{1-\eta/2} e^{\left(V^{\eta} + 2\beta V^{\eta/2}\right)}$	Proposed
Case B	$\dot{V} \leq -\frac{1}{\eta T_c} \exp[V^{\eta}] V^{1-\eta}, \forall x \neq 0$	[31]
Case C	$\dot{V} \leq -\frac{\pi}{\eta \mu T_{\mathrm{c}}}\left[V^{1-\frac{\eta}{2}} + \beta^2 V^{1+\frac{\eta}{2}}\right]$	[24]
Case D	$\dot{V} \leq \frac{-\pi}{\eta T_c}\left(V^{1-\frac{\eta}{2}} + V^{1+\frac{\eta}{2}}\right)$	[23]

The evaluation focuses on key performance criteria, including attitude tracking errors, angular velocity behavior, sliding surface evolution, uncertainty estimation accuracy, and the required control effort, both with and without the time-delay-estimation-based compensator. The parameter values used in all simulations are listed in Table (3).

Figure (1) compares the convergence of the proposed Lyapunov function with three Lyapunov functions selected from other reputable references for the simulation parameters $T_c = 5$, $\eta = 0.5$, and $\beta = 2$. As can be seen, the proposed Lyapunov function exhibits superior performance in both convergence speed and steady-state accuracy.

Figure (2) presents the time response of the proposed Lyapunov function described in Eq. (36) for several different initial conditions, considering a predefined convergence time of 5 seconds. As shown, the function converges in all cases within a time shorter than the prescribed upper bound.

Table (3): Parameters used for simulating the proposed control system

$\boldsymbol{\sigma}(0) = [-0.7, 0.2, 0.4]^{\mathrm{T}}$	$\omega(0) = [-0.03 \quad 0.02 \quad -0.01]^{T}$ rad/s	$J_0 = \begin{bmatrix} 20 & 1.2 & 0.9 \\ 1.2 & 7 & 1 \\ 0.9 & 1.4 & 5 \end{bmatrix}$
$R = 500km, \mu_g = 3.986 \times 10^{14}$ $\omega_o = \sqrt{\frac{\mu_g}{R^3}}$	$d(t) = \begin{bmatrix} 0.03 + 0.05\sin(\omega_o t) - 0.03\cos(\omega_o t) \\ 0.04 - 0.02\sin(\omega_o t) + 0.05\cos(\omega_o t) \\ 0.05 - 0.04\sin(\omega_o t) + 0.05\cos(\omega_o t) \end{bmatrix} + 0.5 \times \mathrm{rand}(3,1)(N \cdot m)$	
$Tc = 4 \; and \; 6 \; sec, \eta = 0.5$	$\lambda = 10$, $\Delta_D = 0.5$	

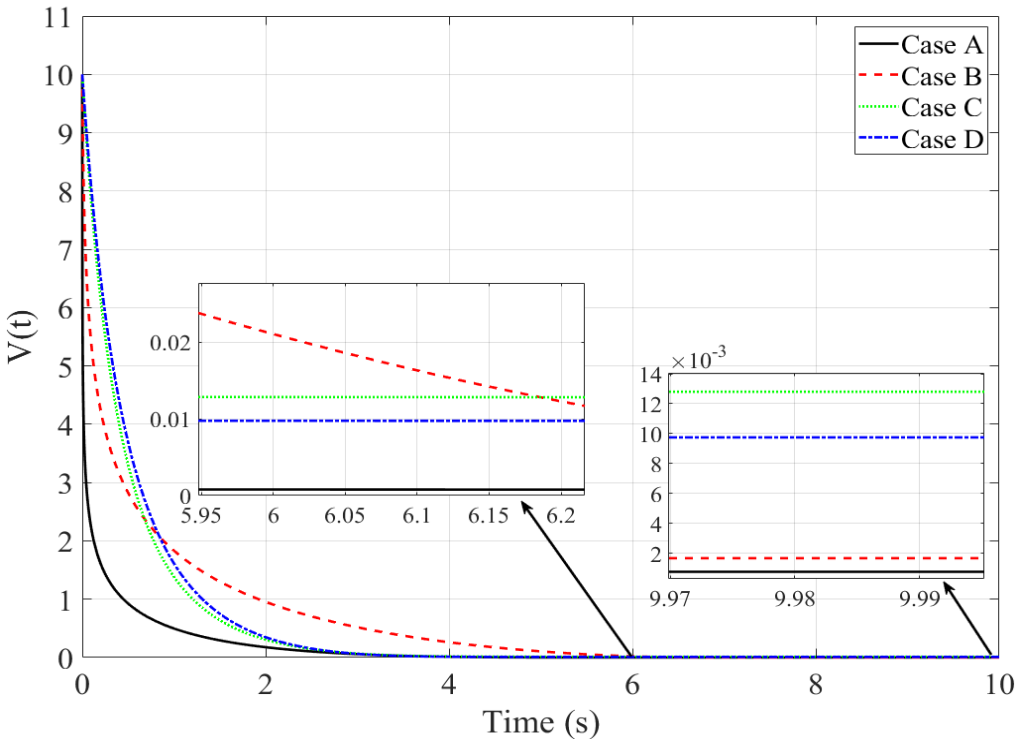


Figure (1): Time evolution of the predefined-time Lyapunov function under different initial conditions.

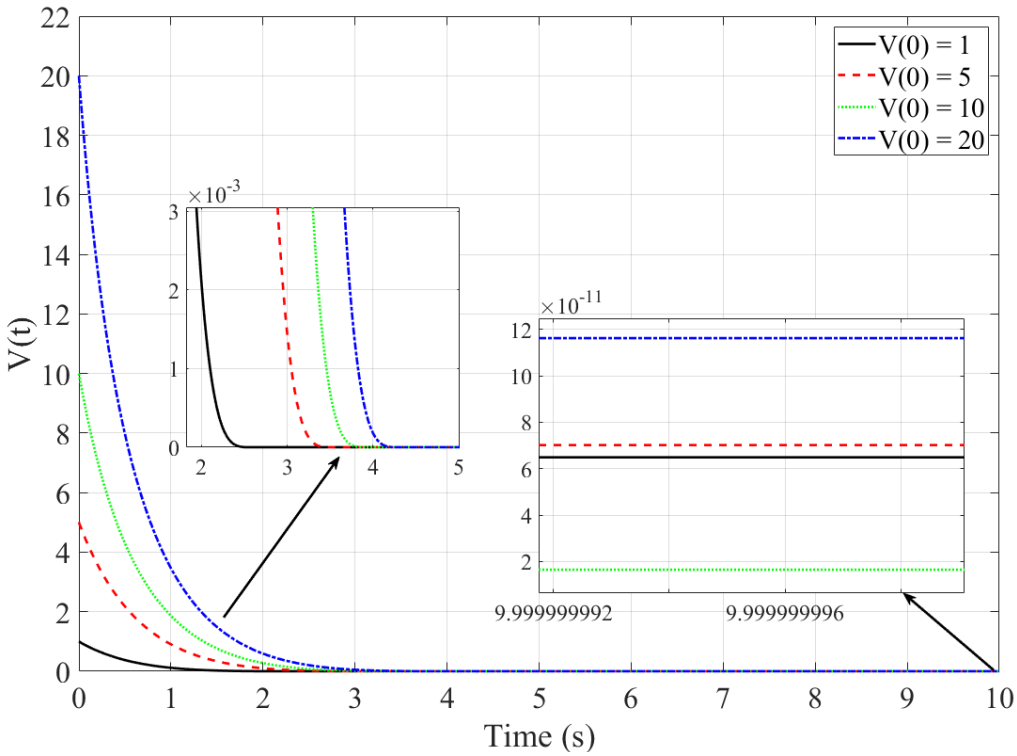


Figure (2): Time evolution of the proposed Lyapunov function with a prescribed convergence time under different initial conditions

Figure (3) illustrates how the adjustable power parameter ηaffects both the accuracy and the convergence rate of the Lyapunov function. In general, this parameter plays a key role in shaping the system's behavior: increasing its value enhances the convergence speed and reduces the steady-state error, which is beneficial for control performance. However, since this parameter also influences the control input, selecting excessively large values may lead to control efforts that exceed actuator constraints. The appropriate

selection of this parameter depends on factors such as the system dynamics, the expected initial conditions of the Lyapunov function, and the desired stability time. In practice, values between 0 and 1 (e.g., 0.5) typically provide a suitable balance, ensuring the required accuracy and convergence rate without imposing excessive stress on the actuators.

Figure (4) demonstrates the convergence results of the proposed Lyapunov function for various values of the adjustable parameter $\beta$and specified predefined convergence times. As observed from the figure, the convergence rate of the Lyapunov function increases with the parameter β. Therefore, this parameter can be adjusted to tune the convergence speed according to the requirements of the specific problem, allowing for the determination of an optimal value based on the control objective.

Figure (5) presents the convergence results of the proposed Lyapunov function for specific adjustable parameters and different predefined convergence times. It is evident from this figure that for any predefined time specified by the control system designer, the proposed Lyapunov function converges within a time frame shorter than the designated limit, independent of initial conditions and control design parameters.

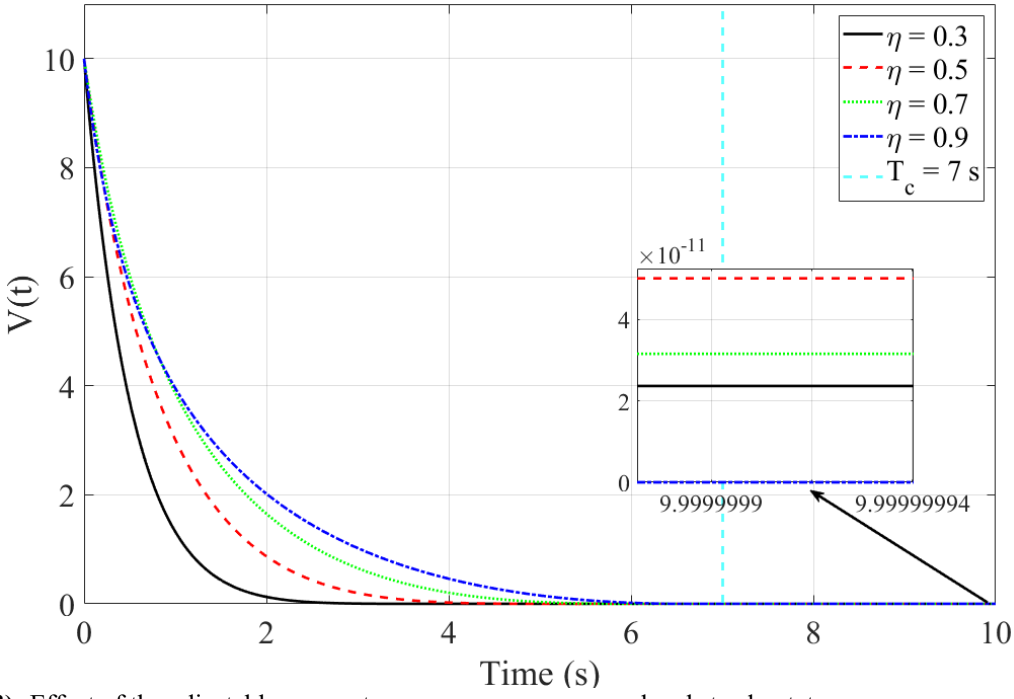


Figure (3): Effect of the adjustable parameter ηon convergence speed and steady-state convergence error.

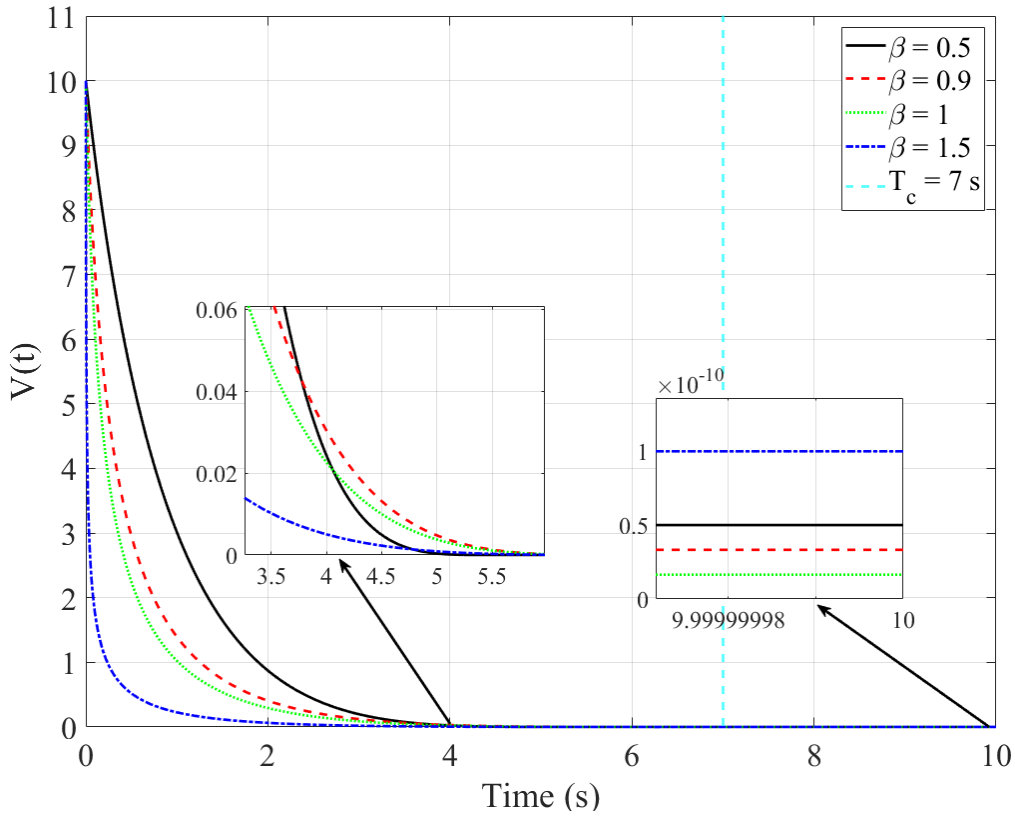


Figure (4): Effect of the adjustable parameter β on convergence speed and steady-state convergence error.

562

563

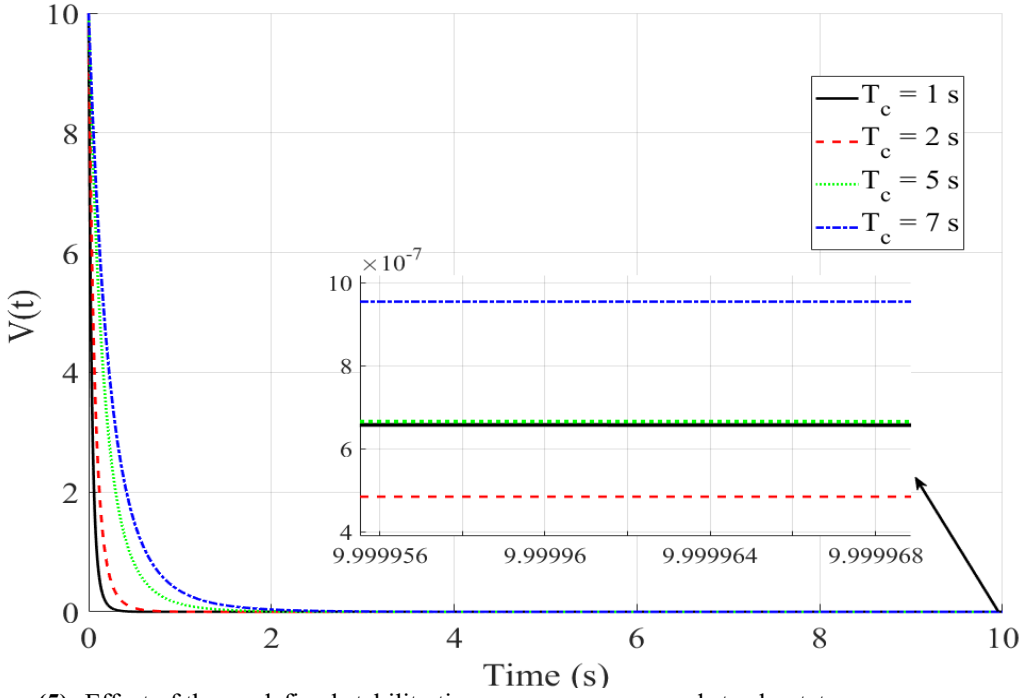


Figure (5): Effect of the predefined stability time on convergence and steady-state convergence error.

564

565 Figure (6) depicts the operational predefined-time stability region obtained from Eq. (63). As shown, even in the presence of
566 uncertainty, the proposed Lyapunov function converges to a bounded region after a finite time interval shorter than the prescribed
567 time. This confirms that the proposed formulation preserves operational predefined-time convergence under uncertain conditions.

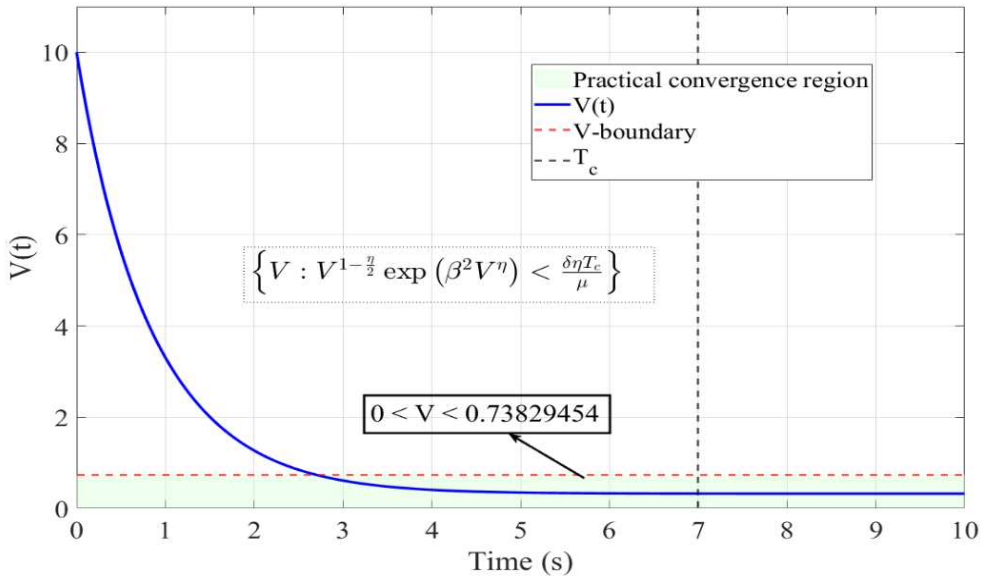


Figure (6): Practical stability region of the proposed Lyapunov function for an uncertainty level of $\delta = 0.5$

Figure (7) illustrates the operational convergence region of the proposed Lyapunov function for different uncertainty levels. As observed, increasing the uncertainty magnitude enlarges the operational convergence region; nevertheless, this region remains bounded. Therefore, it can be concluded that, despite the presence of uncertainties and estimation errors, the proposed Lyapunov function retains its predefined-time convergence property.

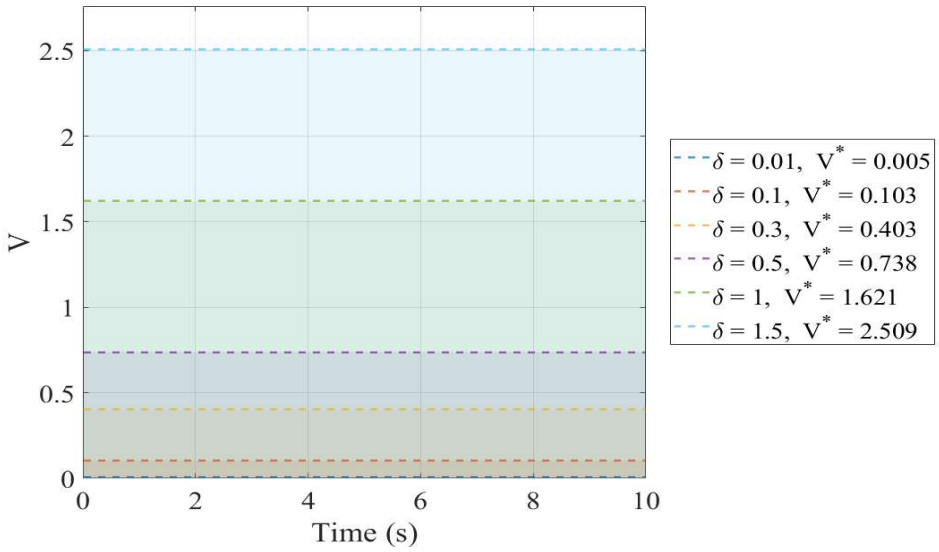


Figure (7): Practical stability region of the proposed Lyapunov function for different uncertainty levels

Figure (8) illustrates the convergence region of the 4 Lyapunov functions listed in Table (2), which were used for comparison under identical parameters in the operational state. As the figure demonstrates, the convergence region of the proposed method is not only smaller in the presence of uncertainty but also converges to this region more rapidly. This indicates that the proposed method exhibits superior robustness and faster reaction speeds when facing uncertainties, offering better performance than other methods in controlling systems affected by uncertainties and external disturbances.

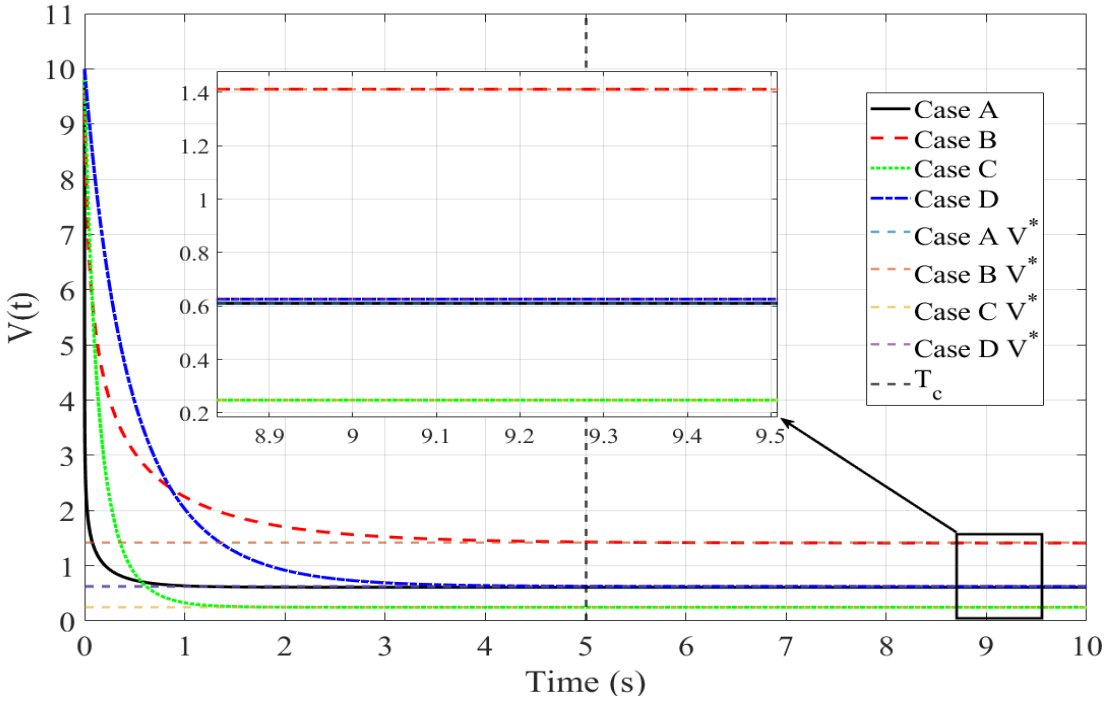


Figure (8): Comparison of the operational convergence region of the proposed Lyapunov function with other similar functions.

Figure (9) shows the time evolution of tracking errors in Modified Rodrigues Parameters (MRP). These results clearly prove that the controller can accurately track the desired state trajectory. After a brief transient period, the errors converge rapidly to zero; this reflects the predefined-time stability property, which guarantees finite-time convergence. The smooth decay of the error also indicates that the controller is effectively capable of handling disturbances and uncertainties. To further validate this feature, the results are displayed alongside 3 other predefined-time stability functions from various sources, with a predefined convergence time of 3 seconds, confirming that the proposed controller achieves better performance in terms of accuracy and convergence speed.

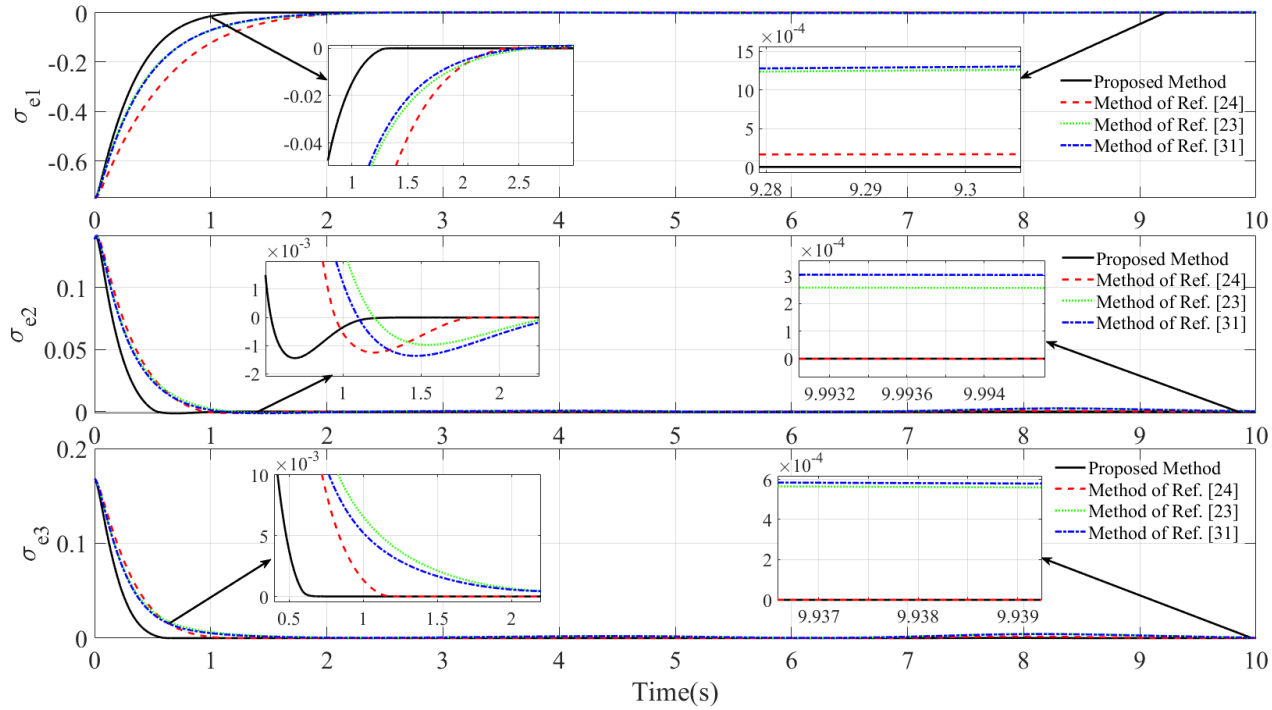


Figure (9): Time evolution of MRP tracking errors ($T_c = 3$).

Figure (10) shows the time evolution of the sliding surfaces. In sliding-mode control, these surfaces are essential because they ensure that the system follows the desired trajectory. The curves initially start far from zero but rapidly move toward the horizontal axis, confirming that the system reaches the sliding manifold within the prescribed time. After completion of the reaching phase, the system states remain confined to the sliding manifold. The smooth transition also indicates that the chattering phenomenon has been effectively mitigated, which is a significant advantage for real-world implementation.

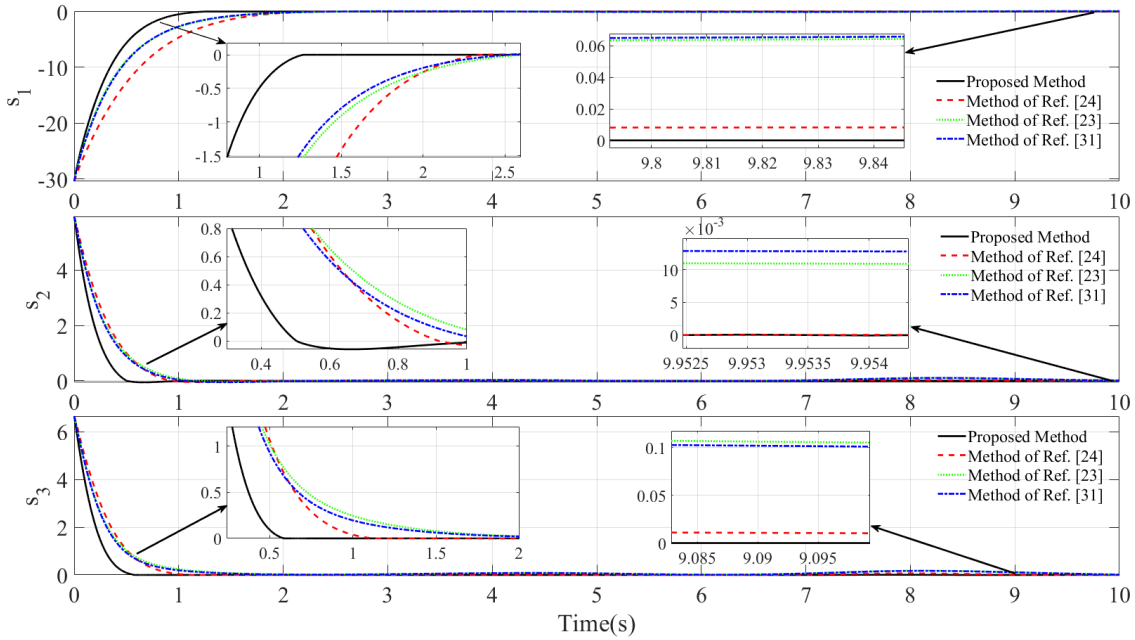


Figure (10): Time evolution of the sliding surface ($T_c = 3$).

Figure (11) presents the time histories of the angular-velocity tracking errors. The results clearly demonstrate the accuracy of the controller, as the errors rapidly converge to zero. The smooth decreasing trend, with no significant oscillations, indicates that the controller successfully regulates the satellite's rotational motion while effectively compensating for external disturbances and model uncertainties.

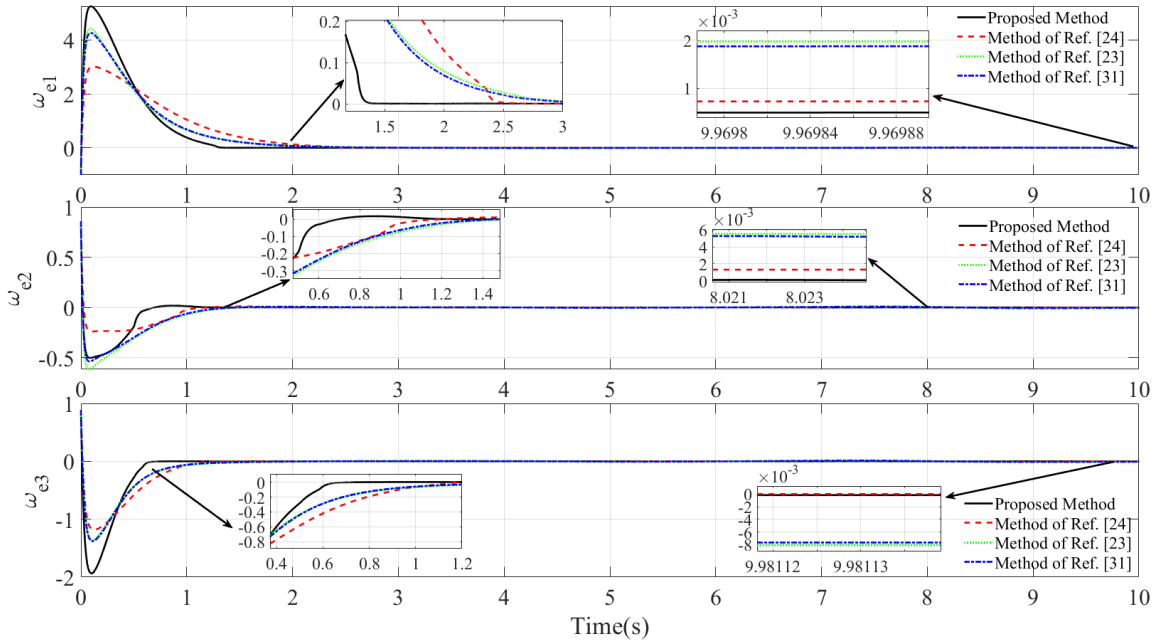


Figure (11): Time histories of the angular-velocity tracking errors ($T_c = 3$).

Figures (12) and (13) illustrate the performance of the time-delay-estimation method in estimating the lumped system uncertainties. In Figure (12), the estimated uncertainties closely follow the expected behavior, indicating that the estimator effectively identifies the unknown system dynamics. Figure (13) presents the estimation errors, defined as the difference between the actual and estimated uncertainties, which remain negligible. This confirms that the proposed estimator provides an accurate and real-time approximation of the disturbances and model uncertainties.

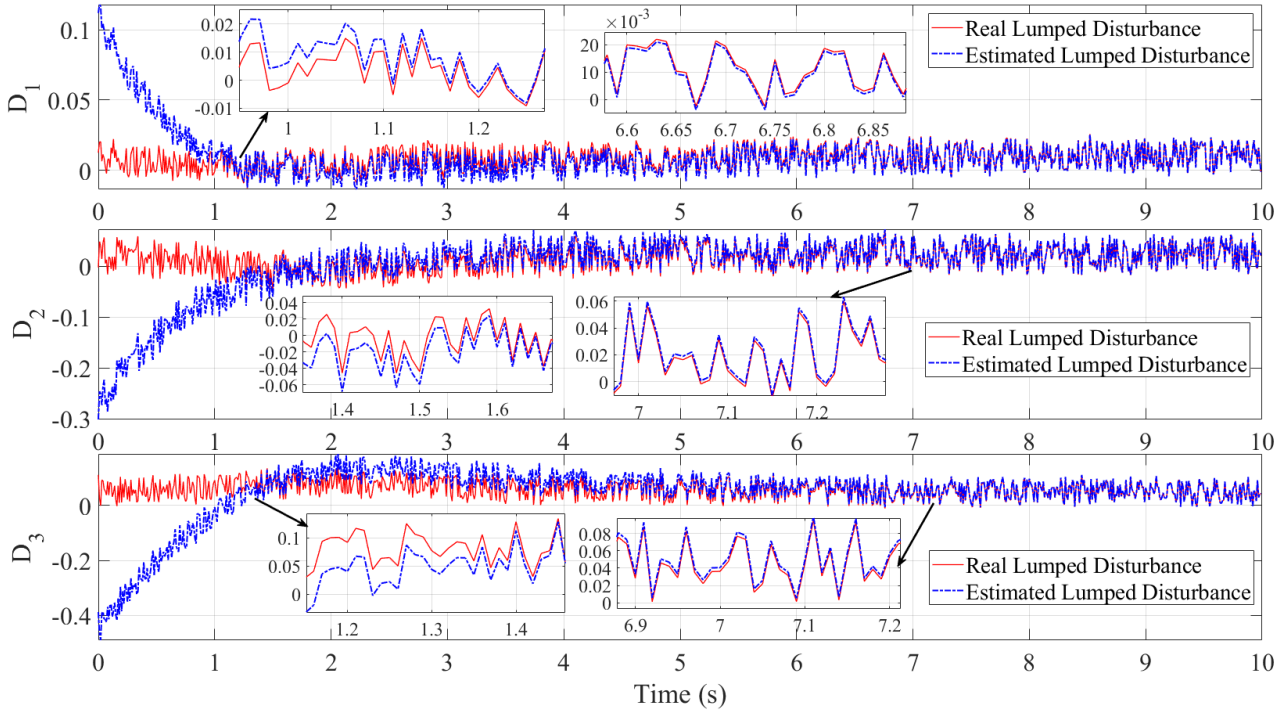


Figure (12): Performance of the time-delay-estimation method in estimating the lumped system uncertainty.

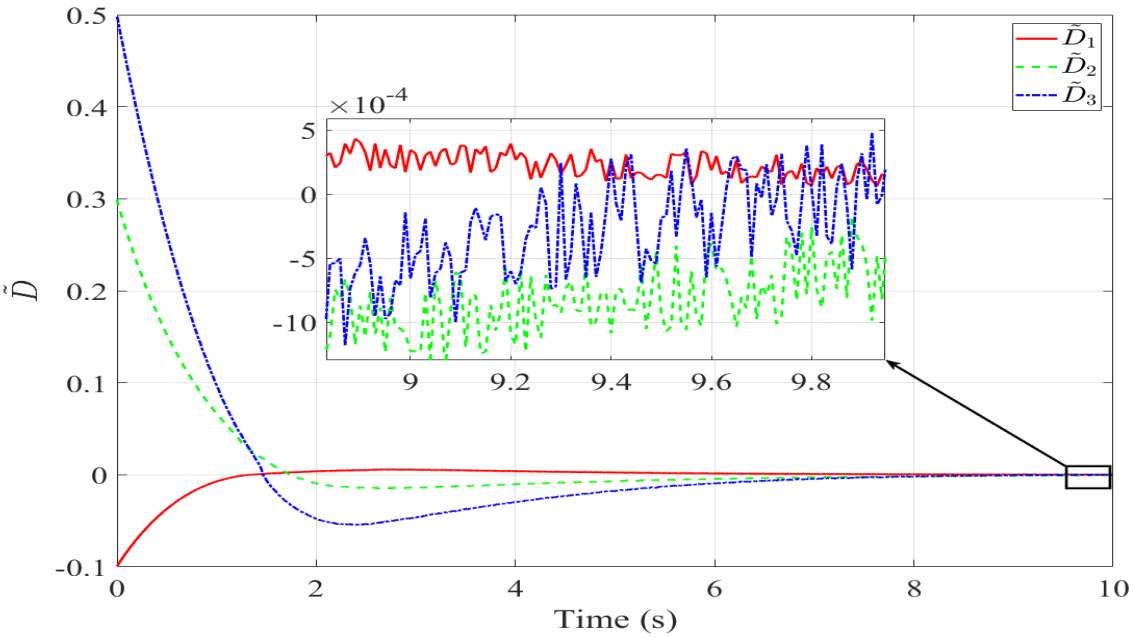


Figure (13): Estimation error of the lumped system uncertainty.

Figure (14) depicts the time evolution of the control inputs and provides a clear perspective on the effect of control effort on system performance. As observed, the control signals generated by the compared methods have larger amplitudes and exhibit noticeable oscillations. In contrast, incorporating the time-delay-estimation-based compensator into the proposed method produces smoother

control inputs with reduced magnitudes. This demonstrates the benefit of integrating the time-delay estimator, as it not only ensures accurate tracking but also reduces the required control effort, thereby resulting in a more energy-efficient control strategy.

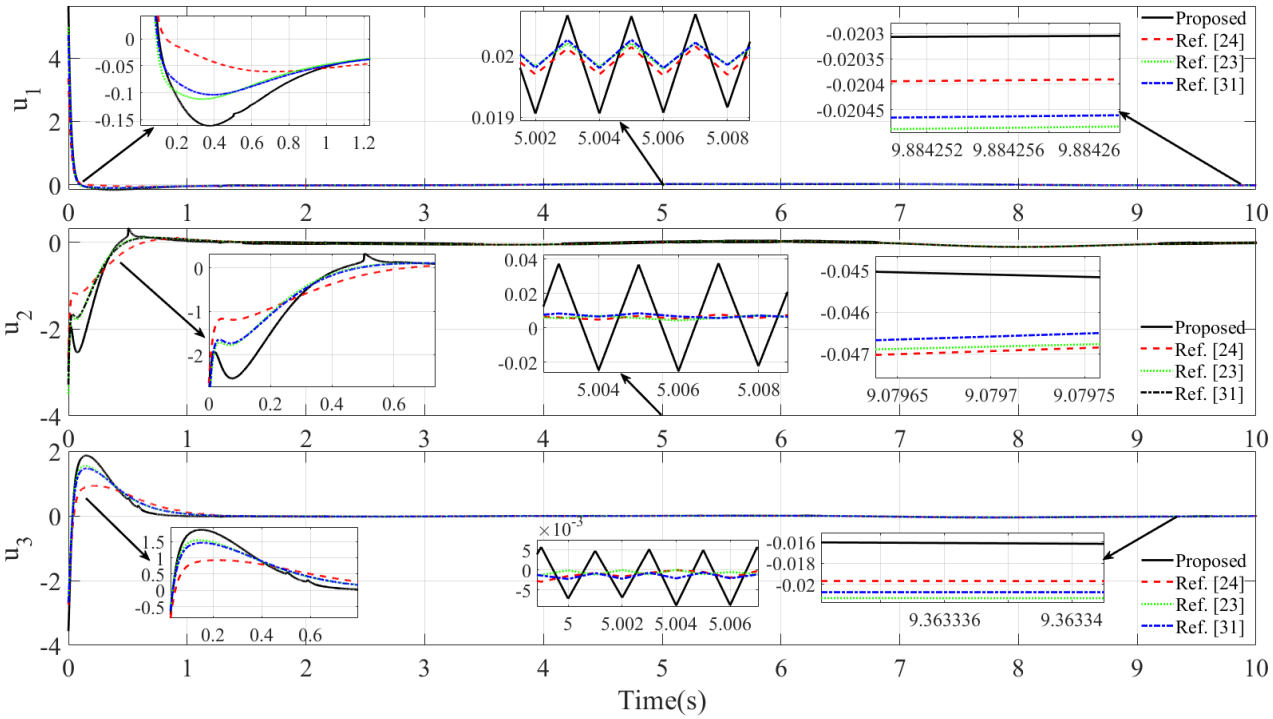


Figure (14): Time histories of the control inputs generated by the proposed method and the comparative methods.

Conclusion

The simulation results demonstrate that the proposed sliding-mode controller, combined with the time-delay-estimation-based method, provides effective satellite attitude control with a predefined-time stability guarantee. Predefined-time stability ensures that the tracking errors converge within a prescribed fixed time, independently of their initial values, initial conditions, and controller parameters. Integrating the time-delay estimator enables accurate estimation of the effects of external disturbances and dynamic uncertainties, thereby reducing the required control effort and smoothing the control signals through the design of compensatory control inputs. In addition, the results indicate that the chattering phenomenon is effectively mitigated, making the proposed approach suitable for practical satellite attitude-control applications.

Overall, the key findings of this study can be summarized as follows:

1. The controller achieves convergence of the attitude-tracking errors within the prescribed time, independently of the initial conditions and controller parameters.
2. Operational predefined-time stability is maintained in the presence of the time-delay-estimation method.
3. The sliding surfaces confirm that the sliding-mode condition required for predefined-time convergence is effectively satisfied.
4. The angular-velocity tracking errors rapidly converge to zero, demonstrating accurate tracking performance.
5. The time-delay-based estimator accurately identifies the lumped uncertainties with a bounded estimation error.
6. Applying the time-delay-estimation-based compensatory control input reduces the required control effort and improves the smoothness of the control signals.

In conclusion, the proposed method provides a robust, accurate, and energy-efficient solution for satellite attitude control in the presence of uncertainties and external disturbances, even when stochastic terms are considered in the modeling of unknown external disturbances.

Declaration of interests

The authors declare that they have no known competing financial interests or personal relationships that could have appeared to influence the work reported in this paper.

Funding Declaration

The authors declare that no financial support or funding was received from any organization, institution, or funding agency for the conduct of this research or the preparation of this manuscript. This study was conducted solely as part of an academic research activity.

References

[1] N. Nazari, H. Moladavoudi, and J. Beyramzad, "Finite time sliding mode control for agile rigid satellite with CMG actuators using fast high-order sliding mode observer," *Aerosp. Syst.*, vol. 7, no. 2, pp. 363–383, 2024.

[2] J. Beyramzad, K. Daneshjoo, and E. Khanmirza, "Extreme learning machine based intelligent robust nonsingular practical tunable predefined-time stable sliding mode attitude control of uncertain space systems," *Adv. Sp. Res.*, 2026.

[3] H. Akherati, J. Beyramzad, S. S. Khiyabani, A. Shariatinezhad, and E. Eskandari, "Finite-time stable model free sliding mode attitude controller/observer design for uncertain space systems based on time delay estimation," *Adv. Sp. Res.*, vol. 76, no. 6, pp. 3573–3594, 2025.

[4] J. Beyramzad, K. Daneshjou, and E. Khanmirza, "Design a finite-time chattering free attitude controller for rigid spacecraft's without angular velocity measurement using interval type-II fuzzy logic nonsingular terminal sliding mode and nonlinear extended state observer," in *21 st International Conference of Iranian Aerospace Society*, 2023, pp. 1–8.

[5] H. Yadegari, J. Beyramzad, and E. Khanmirza, "Magnetorquers-based satellite attitude control using interval type-II fuzzy terminal sliding mode control with time delay estimation," *Adv. Sp. Res.*, vol. 69, no. 8, pp. 3204–3225, 2022.

[6] S. M. Sadigh, A. Kashaninia, and S. M. M. Dehghan, "Adaptive finite-time fault-tolerant control for nano-satellite attitude tracking under actuator constraints," *Aerosp. Sci. Technol.*, vol. 138, p. 108337, 2023.

[7] S. Piri, J. Beyramzad, and E. Khanmirza, "Finite-Time Disturbance Observer Based Fractional Order Nonsingular Terminal Sliding Mode Attitude Control of Satellites," *J. Sp. Sci. Technol.*, vol. 17, no. Special Issue (S1), pp. 45–58, 2024.

[8] H. Soleymani, M. Bakhtiari, and J. Beyramzad, "A Fixed-time Stable Output Feedback Non-singular Fast Terminal Sliding Mode Design for Attitude Control of a Rigid Spacecraft Considering External Disturbances and System Uncertainties," *J. Sp. Sci. Technol.*, vol. 18, no. 2, pp. 70–82, 2025.

[9] M. Bakhtiari, S. A. Kazemi, J. Beyramzad, and A. Panahyazdan, "Nonlinear Control of Two Non-Cooperative Spacecraft for Orbital Rendezvous and Proximity Operations Using a Sliding Mode Controller and a Third-Order Sliding Mode Observer with Finite-Time Convergence," *J. Technol. Aerosp. Eng.*, vol. 10, no. 1, pp. 15–26, 2026.

[10] A. Hemmati, N. M. R. Sayyed, and J. Beyramzad, "Dynamic Modeling and Developing a Sliding Mode Controller Based on a Fixed-Time Disturbance Observer for Simultaneous Control of Distance and Attitude in Spacecraft Proximity Operations," 2025.

[11] A. Y. Aleksandrov and A. A. Tikhonov, "Application of a PID-like control to the problem of triaxial electrodynamic attitude stabilization of a satellite in the orbital frame," *Aerosp. Sci. Technol.*, vol. 127, p. 107720, 2022.

[12] D. Lee, "Nonlinear disturbance observer-based robust control of attitude tracking of rigid spacecraft," *Nonlinear Dyn.*, vol. 88, no. 2, pp. 1317–1328, 2017.

[13] B. Baghi, M. Kabganian, R. Nadafi, and E. Arabi, "Three-axis attitude stabilization of a flexible satellite using non-linear PD controller," *Trans. Inst. Meas. Control*, vol. 40, no. 2, pp. 591–605, 2018.

[14] Q. Yao, "Robust adaptive iterative learning control for high-precision attitude tracking of spacecraft," *J. Aerosp. Eng.*, vol. 34, no. 1, p. 4020108, 2021.

[15] Y. Guo, B. Huang, S. Song, A. Li, and C. Wang, "Robust saturated finite-time attitude control for spacecraft using integral

sliding mode," *J. Guid. Control. Dyn.*, vol. 42, no. 2, pp. 440–446, 2019.

[16] M. Ezabadi and S. A. Emami, "Finite-time fault-tolerant control of a spacecraft using composite learning in the presence of moment of inertia uncertainty and external disturbances," *Aerosp. Sci. Technol.*, vol. 150, p. 109185, 2024.

[17] Q. Yao, "Robust finite-time control design for attitude stabilization of spacecraft under measurement uncertainties," *Adv. Sp. Res.*, vol. 68, no. 8, pp. 3159–3175, 2021.

[18] T. Guan, K. Zhang, B. Li, X. Guan, and K.-F. C. Yiu, "Adaptive fixed-time sliding mode control for spacecraft reorientation with attitude pointing constraints and disturbance rejection," *ISA Trans.*, vol. 143, pp. 50–58, 2023.

[19] M. Zhuang and S. Song, "Fixed-time fault-tolerant attitude control for rigid spacecraft with torque saturation," *ISA Trans.*, vol. 139, pp. 229–243, 2023.

[20] Ö. Bingöl, "Attitude synchronization of chaotic satellites with unknown dynamics using a neural network based fixed time sliding mode controller," *Adv. Sp. Res.*, vol. 75, no. 3, pp. 3242–3267, 2025.

[21] S. Barman and M. Sinha, "A Novel Nonsingular Fast Fixed-Time Sliding Mode Control and Its Application to Satellite Attitude Control," *Int. J. Robust Nonlinear Control*, vol. 35, no. 6, pp. 2184–2198, 2025.

[22] M. Golestani, S. M. Esmaeilzadeh, and S. Mobayen, "Fixed-time control for high-precision attitude stabilization of flexible spacecraft," *Eur. J. Control*, vol. 57, pp. 222–231, 2021.

[23] D. Ye, A.-M. Zou, and Z. Sun, "Predefined-time predefined-bounded attitude tracking control for rigid spacecraft," *IEEE Trans. Aerosp. Electron. Syst.*, vol. 58, no. 1, pp. 464–472, 2021.

[24] Y.-Y. Wu, W. Liu, J. Zhang, X. Li, and P. Wang, "Tunable predefined-time attitude tracking control for rigid spacecraft," *IEEE Trans. Circuits Syst. II Express Briefs*, vol. 71, no. 9, pp. 4271–4275, 2024.

[25] H.-J. Sun, Y.-Y. Wu, and J. Zhang, "A distributed predefined-time attitude coordination control scheme for multiple rigid spacecraft," *Aerosp. Sci. Technol.*, vol. 133, p. 108134, 2023.

[26] S. Xie, Q. Chen, and X. He, "Predefined-time approximation-free attitude constraint control of rigid spacecraft," *IEEE Trans. Aerosp. Electron. Syst.*, vol. 59, no. 1, pp. 347–358, 2022.

[27] Y. Su and S. Shen, "Adaptive predefined-time fault-tolerant attitude tracking control for rigid spacecraft with guaranteed performance," *Acta Astronaut.*, vol. 214, pp. 677–688, 2024.

[28] S. Xie and Q. Chen, "Adaptive nonsingular predefined-time control for attitude stabilization of rigid spacecrafts," *IEEE Trans. Circuits Syst. II Express Briefs*, vol. 69, no. 1, pp. 189–193, 2021.

[29] Y. Xiao, Y. Wang, D. Ye, and Z. Sun, "Predefined-time robust attitude tracking control of flexible spacecraft with continuous and nonsingular performance," *Aerosp. Sci. Technol.*, vol. 159, p. 110000, 2025.

[30] Y. Xu, A. Wu, and R. Dong, "Anti-unwinding attitude maneuver control with predefined time for rigid spacecraft with input saturation," *Int. J. Robust Nonlinear Control*, vol. 34, no. 13, pp. 8919–8944, 2024.

[31] F. Wang, Y. Miao, C. Li, and I. Hwang, "Attitude control of rigid spacecraft with predefined-time stability," *J. Franklin Inst.*, vol. 357, no. 7, pp. 4212–4221, 2020.

[32] Z. Zhang, S. Xie, and Q. Chen, "Disturbance observer-based singularity-free predefined-time attitude tracking control of quadrotors: Theory and experiments," *IEEE Trans. Aerosp. Electron. Syst.*, vol. 61, no. 1, pp. 314–324, 2024.

[33] D. Ye, A.-M. Zou, S. Sun, and Y. Xiao, "A predefined-time extended-state observer-based approach for velocity-free attitude control of spacecraft," *IEEE Trans. Aerosp. Electron. Syst.*, vol. 59, no. 6, pp. 8051–8061, 2023.

[34] N. Xuan-Mung, M. Golestani, S. Mobayen, and H. Kong, "Predefined-time disturbance observer-based attitude tracking control for spacecraft: A solution for arbitrary disturbances," *IEEE Trans. Ind. Electron.*, vol. 72, no. 8, pp. 8408–8418, 2025.

[35] J. Chen, Z. Chen, H. Zhang, B. Xiao, and L. Cao, "Predefined-time observer-based nonsingular sliding-mode control for spacecraft attitude stabilization," *IEEE Trans. Circuits Syst. II Express Briefs*, vol. 71, no. 3, pp. 1291–1295, 2023.

[36] Z. Zheng, T. Wang, G. Zhao, and C. Liu, "Nonsingular Predefined-Time Attitude Tracking Control for Rigid Spacecraft with Disturbance Estimation," *IEEE Trans. Aerosp. Electron. Syst.*, 2026.

[37] S. Xie and Q. Chen, "Predefined-time disturbance estimation and attitude control for rigid spacecraft," *IEEE Trans. Circuits Syst. II Express Briefs*, vol. 71, no. 4, pp. 2089–2093, 2023.

[38] Y. Zhang, F. Meng, and Y. Tai, “Neural network-based Predefined-time attitude control for rigid spacecraft with uncertainties and disturbances,” *J. Ind. Manag. Optim.*, vol. 21, no. 3, pp. 1832–1845, 2025.

[39] X. Lu, J. Wang, Y. Wang, and J. Chen, “Neural network observer-based predefined-time attitude control for morphing hypersonic vehicles,” *Aerosp. Sci. Technol.*, vol. 152, p. 109333, 2024.

[40] S. Xie, Q. Chen, and Q. Yang, “Adaptive fuzzy predefined-time dynamic surface control for attitude tracking of spacecraft with state constraints,” *IEEE Trans. Fuzzy Syst.*, vol. 31, no. 7, pp. 2292–2304, 2022.

[41] H. Xu, D. Dong, D. Yu, and Y.-J. Liu, “Predefined-time fuzzy adaptive control for spacecraft pose tracking with asymptotic error,” *IEEE Trans. Fuzzy Syst.*, vol. 33, no. 3, pp. 971–981, 2024.

[42] C.-D. Liang, M.-F. Ge, Z.-W. Liu, G. Ling, and X.-W. Zhao, “A novel sliding surface design for predefined-time stabilization of Euler–Lagrange systems,” *Nonlinear Dyn.*, vol. 106, no. 1, pp. 445–458, 2021.

[43] J. D. Sánchez-Torres, A. J. Muñoz-Vázquez, M. Defoort, R. Aldana-López, and D. Gómez-Gutiérrez, “Predefined-time integral sliding mode control of second-order systems,” *Int. J. Syst. Sci.*, vol. 51, no. 16, pp. 3425–3435, 2020.

[44] M. Zhang, H. Zang, and Z. Shi, “A unified Lyapunov-like characterization for predefined time synchronization of nonlinear systems: M. Zhang et al.,” *Nonlinear Dyn.*, vol. 112, no. 11, pp. 8775–8787, 2024.

[45] A. J. Muñoz-Vázquez, J. D. Sánchez-Torres, S. Gutiérrez-Alcalá, E. Jiménez-Rodríguez, and A. G. Loukianov, “Predefined-time robust contour tracking of robotic manipulators,” *J. Franklin Inst.*, vol. 356, no. 5, pp. 2709–2722, 2019.

[46] Cruz-Zavala E, Moreno JA, Fridman LM. Uniform robust exact differentiator. IEEE Transactions on Automatic Control. 2011 Jun 20;56(11):2727-33.